molecules. The sequences of the synthesized AONs were as follows: h70AON1, 5′-CCACGCUCUCCAGGGAG-3′ and h70AON2, 5′-CUUCCAGGCUCUCCUCGC-3′ for human type VII collagen: hm70AON, 5′-CGCACACUUCCAGGC-3′ for 5818delC mutation (Figures 1a and 5b).

Cell culture and AON transfection

The human keratinocyte HaCaT cell line was maintained in DMEM with 10% fetal bovine serum. Primary keratinocytes were isolated and grown in the presence of mitomycin C-treated 3T3 feeder layer (Rheinwald and Green, 1975). Briefly, keratinocytes, which were obtained from HS-RDEB patient skin biopsies and healthy controls, were cultured on feeder layers of mitomycin C-treated mouse 3T3 fibroblasts in DMEM: Ham's F-12 (3:1) supplemented with 10% fetal bovine serum, 5 μg/ml insulin, 10 ng/ml EGFR, 0.4 μg/ml hydrocortisone, and 8 ng/ml cholera toxin. Human fibroblasts were also obtained from a skin biopsy from an HS-RDEB patient and healthy controls, and were cultured in DMEM with 10% fetal bovine serum. This HS-RDEB patient harbored heterozygous *COL7A1* 5818delC and 1474del8 mutations, and showed no expression of type VII collagen (Goto *et al.*, 2006).

After changing of the medium to serum-free Opti-MEM (Gibco Invitrogen, Grand Island, NY), we transfected the AONs into the cells using Lipofectamine 2000 (Gibco Invitrogen) according to the manufacturer's protocols. In all experiments, the cells were exposed to transfection reagent for 16 hours and the media were replaced with fresh growth medium.

Graft experiments

We transplanted artificial and normal skin onto a nude rat. Briefly, 10^6 HS-RDEB fibroblasts were seeded into a collagen sponge scaffold and maintained in DMEM with 10% fetal bovine serum. Confluent cultures containing 10^6 HS-RDEB keratinocytes were treated with dispase (1 nU/ml; Godo Shusei, Tokyo, Japan), and the floating epidermal sheet placed on the collagen sponge. In nude rats (F344/N Jcl-rnu; CLEA Japan, Tokyo, Japan), the sites for transplantation were prepared by excising a 2 cm^2 area of dorsal skin. The collagen sponge containing the fibroblasts was placed into the skin wound and then the epidermal sheet overlaid on the collagen sponge. In other experiments, normal skin samples were obtained from the abdomens of patients undergoing reconstructive plastic surgery at the Hokkaido University Hospital. Each skin sample was placed directly on the 2 cm^2 wound on the nude rat. Afterwards, an occlusive dressing was quickly placed over the graft to hold it in position and to prevent it from drying. After 7 days, the dressing was removed, and then 30 μg AON was diluted in normal saline to a final volume of 150 μl and injected into several portions of the grafts. After 16 hours, the skin biopsies were taken from the injected site and were subjected to RT-PCR analysis as the *in vitro* time-course study indicated the highest expression of the exon-skipping band at 16 hours after AON transfer.

Informed consents were obtained from all individual subjects in this study. The protocols were approved by the Ethical Committee at Hokkaido University Graduate School of Medicine. This study was conducted according to the Declaration of Helsinki Principles.

RNA isolation and RT-PCR analysis

Skin samples were taken from the rodent model and were first homogenized using a Polytron homogenizer. Total RNA was extracted from skin samples and cultured cells using an RNeasy RNA extraction kit (Qiagen, Hilden, Germany). First strand cDNA was synthesized with reverse transcriptase (Life Sciences, St Petersburg, FL) using an oligo-dT primer. To determine the splice-specific expression of exon 70, we designed the forward PCR primer on the border of exons 65 and 66, and the reversel primer on exon 72. The amplification conditions were carried out using the 66–72 primer set, forward 5′-GAAGGGAGAGAAAGGAGATT-3′ and reversel 5′-GGAAGCTACCAGAGCTCTCA-3′, for 35 cycles of reaction at 94°C for 1 minute, 58°C for 1 minute, and 72°C for 1 minute. In addition, to verify the skipping of exon 70, we set the forward primer on the border of exons 63 and 64, and reversel primer on the border of exons 69 and 71. The amplification conditions were carried out with the 70Δ primer set, forward 5′-TGGATTACCGGGAAAGCCAG-3′ and reversel 5′-GATCCACATTCTGCTCCCCT-3′, for 35 cycles of reaction at 94°C for 1 minute, 58°C for 1 minute, and 72°C for 1 minute. The PCR products were fractionated on 2% agarose gels and directly sequenced by di-deoxy dye-terminator method using an automated sequencer (ABI Prism Genetic Analyzer 3100, PE Biosystems, Foster city, CA). When several bands were found, we subcloned the PCR sample into a TA cloning vector (Gibco Invitrogen). After transformation of the bacteria, we picked up 50 colonies and examined the inserts to semiquantify the amounts of the bands. The rate of the lower band to the upper band was expressed as the exon skipping rate. Each value represents the mean±SD of four samples. Moreover, the PCR products were directly sequenced by di-deoxy dye-terminator method using an automated sequencer (ABI Prism Genetic Analyzer 3100, PE Biosystems, Foster city, CA).

Immunostaining and Western blot analysis. Cultured, transfected cells were fixed with 2% paraformaldehyde in phosphate-buffered saline, and were then incubated with the mAb LH7.2 against the NC1 domain of collagen type VII (Chemicon, Temecula, CA). The secondary antibody was FITC-conjugated goat anti-mouse IgG and preparations were examined under a fluorescence microscope. Subconfluent keratinocyte cultures were fed for 48 hours with serum-free medium supplemented with 50 μg/ml ascorbic acid. For SDS-PAGE analysis, the culture medium was treated with Amicon Ultra-100,000 Centrifugal Filter Devices (Millipore, Bedford, MA) for protein concentration and desalting. The samples were separated on a 5% polyacrylamide gel under reducing conditions. Immunoblotting analysis was performed using the LH7.2 mAb followed by the secondary antibody goat anti-mouse IgG conjugated to peroxidase. The resultant complexes were processed for Phototope horse radish peroxidase Western Blot Detection System (Cell Signaling, Beverly, MA) according to the manufacturer's protocol.

Assays for the type VII collagen without exon 70

Introduction of h70AON2 into keratinocytes induced skipping of exon 70 (see the Results section). We prepared cDNA from the introduced keratinocytes and amplified cDNA without exon 70 (*COL7A1*Δ70). A retroviral vector pDON(Δ) was created by removing the Simian virus-40 promoter and *Neo* gene from pDON-AI (Takara, Kyoto, Japan). The genes *COL7A1* and *COL7A1*Δ70 were inserted into pDON(Δ) and these retrovirus plasmids were introduced into the amphotropic amphopack-293 packaging cells (Clontech, Palo Alto, CA) using calcium phosphate co-precipitation.

The viral particles were recovered from the cell culture medium 48 hours later and applied to cultured DEB keratinocytes that failed to express *COL7A1*. The supernatant of the cultured keratinocytes and the keratinocytes themselves were used for *in vitro* and *in vivo* studies.

The methods for the cell migration assay and cell adhesion assay were performed as described previously (Tsuda *et al.*, 2002). Briefly, culture dishes were treated with conditioned supernatants from cultured HS-RDEB keratinocytes transduced with *COL7A1* and *COL7A1*Δ70 for 24 hours. Control dishes were treated with culture medium. After the plating of normal keratinocytes for 48 hours on the treated dishes, the cells were scraped off using a 200 μl yellow pipette tip. Subsequently, at 8, 16, and 24 hours, the number of cells that had moved from the base line into the scratched area was measured. In addition, normal keratinocytes were allowed to attach for 1.5 hours on the treated dishes and, after removal of unattached cells, washed and fixed with 70% ethanol for 10 minutes. Adherent cells were then stained with crystal violet and the number of the cells was measured.

The collagen sponge containing HS-RDEB fibroblasts was placed on skin wound of nude rat and the confluent cultures of 10^6 HS-RDEB keratinocytes transduced with *COL7A1* and *COL7A1*Δ70 were overlaid on the collagen sponge, as mentioned above. After 8 weeks, the skin biopsies were taken from the graft and subject to routine ultrastructural analysis.

CONFLICT OF INTEREST

The authors state no conflict of interest.

ACKNOWLEDGMENTS

This work was supported in part by Grants-in-Aid from the Ministry of Education, Science, Sports, and Culture of Japan to Sawamura D. (15390337, 17659331) and Shimizu H. (15390336, 17209038), and by grants from the Ministry of Health of Japan to Shimizu H. (H16-Intractable Disease-05).

REFERENCES

Burgeson RE (1993) Type VII collagen, anchoring fibrils, and epidermolysis bullosa. *J Invest Dermatol* 101:252–5

Chen M, Kasahara N, Keene DR, Chan L, Hoeffler WK, Finlay D *et al.* (2002) Restoration of type VII collagen expression and function in dystrophic epidermolysis bullosa. *Nat Genet* 32:670–5

Christiano AM, Greenspan DS, Lee S, Uitto J (1994a) Cloning of human type VII collagen, complete primary sequence of the alpha 1(VII) chain and identification of intragenic polymorphisms. *J Biol Chem* 269: 20256–62

Christiano AM, Hoffman GG, Chung-Honet LC, Lee S, Cheng W, Uitto J *et al.* (1994b) Structural organization of the human type VII collagen gene (COL7A1) composed of more exons than any previously characterized gene. *Genomics* 21:169–79

Cserhalmi-Friedman PB, McGrath JA, Mellerio JE, Romero R, Salas-Alanis, Paller AS *et al.* (1998) Restoration of open reading frame resulting from skipping of an exon with an internal deletion in the COL7A1 gene. *Lab Invest* 78:1483–92

Dokka S, Cooper SR, Kelly S, Hardee GE, Karras JG (2005) Dermal delivery of topically applied oligonucleotides via follicular transport in mouse skin. *J Invest Dermatol* 124:971–5

England SB, Nicholson LV, Johnson MA, Forrest SM, Love DR, Zubrycka-Gaarn EE *et al.* (1990) Very mild muscular dystrophy associated with the deletion of 46% of dystrophin. *Nature* 343:180–2

Galderisi U, Cascino A, Giordano A (1999) Antisense oligonucleotides as therapeutic agents. *J Cell Physiol* 181:251–7

Goto M, Sawamura D, Ito K, Abe M, Nishie W, Sakai K *et al.* (2006) Fibroblasts show more potential target cells than keratinocytes for COL7A1 gene therapy of dystrophic epidermolysis bullosa. *J Invest Dermatol* 126:766–72

Fine JD, Eady RA, Bauer EA, Briggaman RA, Bruckner-Tuderman L, Christiano A *et al.* (2000) Revised classification system for inherited epidermolysis bullosa: report of the Second International Consensus Meeting on diagnosis and classification of epidermolysis bullosa. *J Am Acad Dermatol* 42:1051–66

Lu QL, Mann CJ, Lou F, Bou-Gharios G, Morris GE, Xue SA *et al.* (2003) Functional amounts of dystrophin produced by skipping the mutated exon in the mdx dystrophic mouse. *Nat Med* 9:1009–14

Mann CJ, Honeyman K, Cheng AJ, Ly T, Lloyd F, Fletcher S *et al.* (2001) Antisense-induced exon skipping and synthesis of dystrophin in the mdx mouse. *Proc Natl Acad Sci USA* 98:42–7

Mayeda A, Hayase Y, Inoue H, Ohtsuka E, Ohshima Y (1990) Surveying cis-acting sequences of pre-mRNA by adding antisense 2′-*O*-methyl oligoribonucleotides to a splicing reaction. *J Biochem* 108:399–405

McGrath JA, Ashton GH, Mellerio JE, Salas-Alanis JC, Swensson O, McMillan JR *et al.* (1999) Moderation of phenotypic severity in dystrophic and junctional forms of epidermolysis bullosa through in-frame skipping of exons containing non-sense or frameshift mutations. *J Invest Dermatol* 113:314–21

Monaco AP, Bertelson CJ, Liechti-Gallati S, Moser H, Kunkel LM (1988) An explanation for the phenotypic differences between patients bearing partial deletions of the DMD locus. *Genomics* 2:90–5

Ortiz-Urda S, Thyagarajan B, Keene DR, Lin Q, Fang M, Calos MP *et al.* (2002) Stable nonviral genetic correction of inherited human skin disease. *Nat Med* 8:1166–70

Rheinwald JG, Green H (1975) Serial cultivation of strains of human epidermal keratinocytes: the formation of keratinizing colonies from single cells. *Cell* 6:331–43

Sawamura D, Goto M, Yasukawa K, Sato-Matsumura N, Nakamura H, Ito K *et al.* (2005) Genetic studies of 20 Japanese families of dystrophic epidermolysis bullosa. *J Hum Genet* 50:543–6

Tamai K, Murai T, Mayama M, Kon A, Nomura K, Sawamura D *et al.* (1999) Recurrent COL7A1 mutations in Japanese patients with dystrophic epidermolysis bullosa: positional effects of premature termination codon mutations on clinical severity. *J Invest Dermatol* 112:991–3

Terracina M, Posteraro P, Schubert M, Sonego G, Atzori F, Zambruno G *et al.* (1998) Compound heterozygosity for a recessive glycine substitution and a splice site mutation in the COL7A1 gene causes an unusually mild form of localized recessive dystrophic epidermolysis bullosa. *J Invest Dermatol* 111:744–50

Tsuda M, Tanaka S, Sawa H, Hanafusa H, Nagashima K (2002) Signaling adaptor protein v-Crk activates Rho and regulates cell motility in 3Y1 rat fibroblast cell line. *Cell Growth Differ* 13:131–9

Uitto J, Chung-Honet LC, Christiano AM (1992) Molecular biology and pathology of type VII collagen. *Exp Dermatol* 1:2–11

Uitto J, Hovnanian A, Christiano AM (1995) Premature termination codon mutations in the type VII collagen gene (COL7A1) underlie severe recessive dystrophic epidermolysis bullosa. *Proc Assoc Am Phys* 107:245–52

Wessagowit V, Kim SC, Woong Oh S, McGrath JA (2005) Genotype-phenotype correlation in recessive dystrophic epidermolysis bullosa: when missense doesn't make sense. *J Invest Dermatol* 124:863–6

Zuker M (2003) Mfold web server for nucleic acid folding and hybridization prediction. *Nucleic Acids Res* 31:3406–15

doi: 10.1111/j.1365-2230.2006.02260.x

Eccrine porocarcinoma and Bowen's disease arising in a seborrhoeic keratosis

D. Hoshina, M. Akiyama, H. Hata, S. Aoyagi, K. C. Sato-Matsumura and H. Shimizu

Department of Dermatology, Hokkaido University Graduate School of Medicine, Sapporo, Japan

Summary

An association between seborrhoeic keratosis (SK) and malignant tumours is considered to be rare. We observed a case of eccrine porocarcinoma and Bowen's disease (BD) occurring synchronously, forming one lesion in a SK on the abdomen. It is controversial whether malignant neoplasms arising in SK occur only by chance or if pre-existing SK plays a role in pathogenesis. This case suggests an implication of pre-existing SK in the subsequent development of both BD and eccrine porocarcinoma.

Although the association between seborrhoeic keratosis (SK) and malignant skin tumours within one lesion has been reported since 1932,[1,2] this is generally considered a rare combination. Most malignant tumours reported to occur within an SK are known to be basal cell carcinomas (BCC).[3] We report a case of eccrine porocarcinoma and Bowen's disease (BD) occurring synchronously, forming a single lesion on a SK of the abdomen.

Report

An 87-year-old Japanese woman was referred for treatment of a skin tumour on her abdomen. She had first noticed a brownish macule on the abdomen several years previously. In the centre of the macule, a small, dark and pinkish-red nodule had been noticed 1 year previously.

Physical examination revealed a regular-shaped, slightly elevated, brownish macule, 18 × 17 mm in size, in the centre of the abdomen. Within the macule, a dark-brown to black, partly reddish nodule, 7 × 5 mm in size, was seen (Fig. 1).

Correspondence: Dr Masashi Akiyama MD, PhD, Department of Dermatology, Hokkaido University Graduate School of Medicine, North 15 West 7, Kita-ku, Sapporo 060-8638, Japan.
E-mail: akiyama@med.hokudai.ac.jp

Conflict of interest: none declared.

Accepted for publication 30 June 2006

An excisional biopsy of the whole lesion revealed three distinct histopathological patterns (Fig. 2a). (i) The brownish macule showed markedly thickened epidermis with pseudohorn cysts and basal melanosis, corresponding to a typical SK (Fig. 2b). (ii) A black area of the small nodule was composed of atypical squamous cells with hyperchromatic nuclei, consistent with BD. Single-cell keratinization and atypical mitotic figures were seen in the tumour-cell nests. No apparent

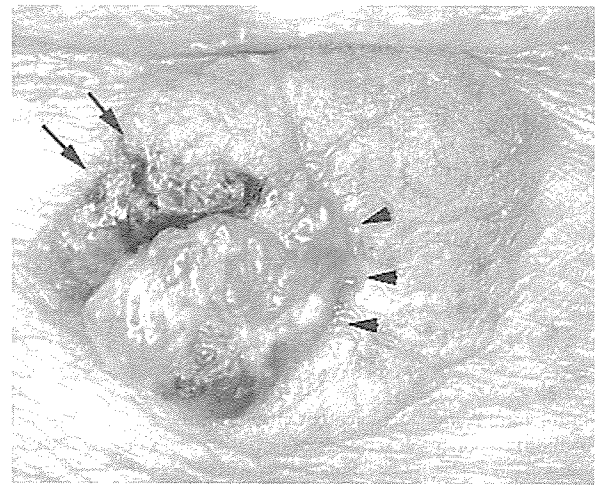

Figure 1 A regular-shaped, slightly elevated, brownish macule in the centre of abdomen. In the macule, a dark-brown to black nodule (arrow) was seen, with the central portion being a reddish colour (arrowhead).

invasion of the tumour beyond the basement membrane was observed (Fig. 2c). Tumour cells in this black area were negative for carcinoembryonic antigen (CEA), and did not stain with alcian blue. (iii) A reddish area of the nodule consisted of atypical cells with hyperchromatic nuclei, consistent with eccrine porocarcinoma. The tumour cells in this area formed irregularly shaped nests of varying size, and secreted mucinous products. In the nests, duct-like structures were seen, forming several cysts (Fig. 2d). Immunohistochemistry showed that this area was positive for CEA (Fig. 2e) and stained with periodic-acid–Schiff (Fig. 2f). Eccrine porocarcinoma is characterized by epidermotropism and pagetoid diffusion in the epidermis, and may show bowenoid changes.[4] However, in this patient, the BD and eccrine porocarcinoma lesions were separated completely by the SK lesion with sufficient distance to allow each lesion to be clearly identified. In addition, tumour cells in the BD lesion were negative for CEA and did not stain with alcian blue. Thus, we believe that the lesion represented true BD rather than bowenoid changes in an eccrine porocarcinoma.

The tumour was diagnosed as BD and eccrine porocarcinoma arising in a SK and was excised with a wide margin. The patient remains asymptomatic after 2 years' follow-up.

In this case, a small nodular lesion composed of BD and eccrine porocarcinoma appeared within a pre-existing elevated macular SK lesion. Several types of malignant neoplasms arising in SK have been reported in the literature.[3,5–9] Most of these malignant tumours are basal cell carcinomas. Some cases of BD and malignant sweat-gland tumours have been reported.[5–9] It is controversial whether malignant neoplasms arising in

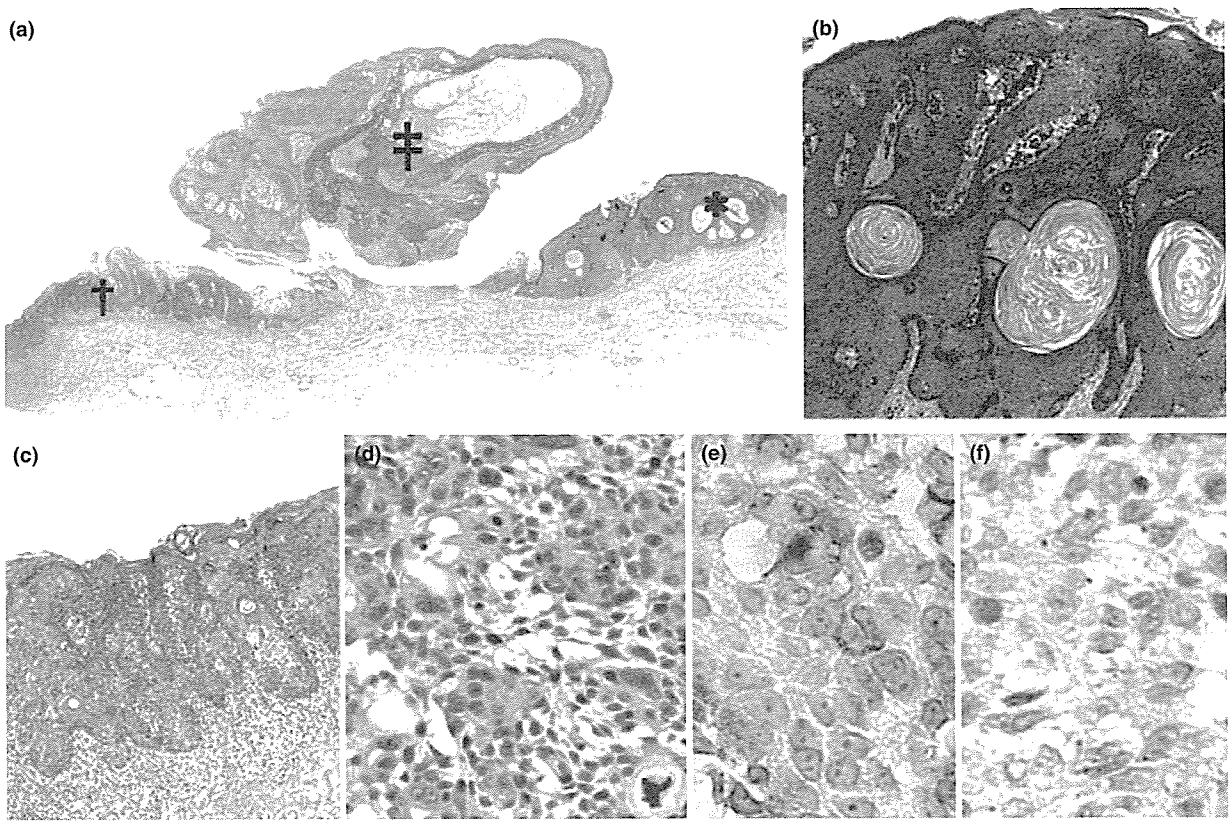

Figure 2 (a) A low-magnification view showing the locations of three compartments of the lesion. Areas with symbols are enlarged in (b–d): (b) *seborrhoeic keratosis (SK); (c) †Bowen's disease (BD); (d) ‡eccrine porocarcinoma. (b) Markedly thickened epidermis with pseudohorn cysts and basal melanosis was seen in the brownish macules (SK lesion). (c) Atypical squamous cells with hyperchromatic nuclei, single-cell keratinization and atypical mitotic figures were apparent in the dark-brown nodule (BD lesion). No apparent invasion of the tumour was seen beyond the basement membrane. (d) Atypical cells with hyperchromatic nuclei formed irregularly shaped nests of varying size and produced mucinous products in the reddish zone of the nodule (region of porocarcinoma). Ductal structures were seen in the nests. Haematoxylin and eosin; original magnification (a) ×25; (b–d) ×100. The cytoplasm of atypical cells showing eccrine-gland differentiation was positive for carcinoembryonic antigen (e) and stained with periodic-acid–Schiff (f) (original magnification ×200 for both).

SK occur only by chance or if pre-existing SK plays a particular role in the pathogenesis of the malignant neoplasms. The present case, in which two different kinds of malignant tumour occurred at the same time within the lesion, implicates the pre-existing SK in the subsequent development of both BD and eccrine porocarcinoma. Altered expression of several proteins associated with cell-cycle regulation and cell proliferation have been reported in SK,[10,11] and such altered patterns of expression may be related to the occurrence of malignant tumours in SK lesions. Further study is necessary to clarify the exact role of pre-existing SK in the subsequent development of secondary malignant tumours.

References

1 Sibley K. Seborrheic verrucae and multiple basal-celled epithelioma. *Proc R Soc Med* 1932; **25**: 670.
2 Sibley K. Seborrheic verrucae and multiple basal-celled epithelioma. *Proc R Soc Med* 1932; **25**: 926.
3 Cascajo CD, Reichel M, Sanchez JL. Malignant neoplasms associated with seborrheic keratoses. *Am J Dermatopathol* 1996; **18**: 273–82.
4 Obi M, Satoh T, Yokozeki H, Nishioka K. Eccrine porocarcinoma with bowenoid changes: epithelial membrane antigen is not a useful marker for malignant tumours arising from eccrine gland structures. *Acta Derm Venereol* 2004; **84**: 142–4.
5 Lozano Orella JA, Valcayo Penalba A, San Juan CC *et al.* Eccrine porocarcinoma: report of nine cases. *Dermatol Surg* 1997; **23**: 925–8.
6 Nagore E, Diaz F, Sanchez-Motilla JM *et al.* A poroid neoplasia arising close to a seborrheic keratosis and trichoepithelioma. *J Dermatol* 1999; **26**: 253–7.
7 Miracco C, Angeloni G, Miracco F *et al.* Carcinoma with eccrine differentiation arising in a seborrheic keratosis. *Br J Dermatol* 2003; **148**: 823–42.
8 Johr R, Saghari S, Nouri K. Eccrine porocarcinoma arising in a seborrheic keratosis evaluated with dermoscopy and treated with Mohs' technique. *Int J Dermatol* 2003; **42**: 653–7.
9 de Giorgi V, Massi D, Sestini S *et al.* Cutaneous collision tumour (melanocytic naevus, basal cell carcinoma, seborrheic keratosis): a clinical, dermoscopic and pathological case report. *Br J Dermatol* 2005; **152**: 787–90.
10 Kamiya M, Takeuchi Y, Katho M *et al.* Expression of p73 in normal skin and proliferative skin lesions. *Pathol Int* 2004; **54**: 890–5.
11 Ko CJ, Shintaku P, Binder SW. Comparison of benign keratoses using p53, bcl-1, and bcl-2. *J Cutan Pathol* 2005; **32**: 356–9.

Short Communication
doi: 10.1111/j.1600-0749.2006.00332.x

Oculocutaneous albinism type 4: six novel mutations in the membrane-associated transporter protein gene and their phenotypes

Katsuhiko Inagaki[1], Tamio Suzuki[1,*], Shiro Ito[1], Noriyuki Suzuki[1], Koji Adachi[2], Torayuki Okuyama[3], Yusei Nakata[4], Hiroshi Shimizu[5], Hironori Matsuura[6], Takashi Oono[6], Hiroko Iwamatsu[7], Michihiro Kono[1] and Yasushi Tomita[1]

[1]Department of Dermatology, Nagoya University Graduate School of Medicine, Nagoya, Japan
[2]Department of Dermatology, Tottori University Faculty of Medicine, Tottori, Japan
[3]Department of Genetics, National Research Institute for Child Health and Development, Tokyo, Japan
[4]Neonatal Intensive Center Unit, Hiroshima Municipal Hospital, Hiroshima, Japan
[5]Department of Dermatology, Hokkaido University Graduate School of Medicine, Sapporo, Japan
[6]Department of Dermatology, Okayama University Graduate School of Medicine, Okayama, Japan
[7]Department of Pediatrics, Oita Prefectural Hospital, Oita, Japan
*Address correspondence to Tamio Suzuki,
e-mail: tasuzuki@med.nagoya-u.ac.jp

Summary

Oculocutaneous albinism type 4 (OCA4) is an autosomal recessive hypopigmentary disorder caused by mutations in the Membrane-Associated Transporter Protein gene (*SLC45A2*). The SLC45A2 protein is a 530-amino-acid polypeptide that contains 12 putative transmembrane domains, and appears to be a transporter that mediates melanin synthesis. Eighteen pathological mutations have been reported so far. In this study, six novel mutations, p.Y49C (c.146A > G), p.G89R (c.265G > A), p.C229Y (c.686G > A), p.T437A (c.1309A > G), p.T440A (c.1318A > G) and p.G473D (c.1418G > A) were found in eight Japanese patients with various clinical phenotypes. The phenotypes of OCA4 were as various as the other types of OCA and probably depended on the mutation sites in the *SLC45A2* gene.

Key words: OCA4/*SLC45A2*/six novel mutations

Received 19 May 2006, revised and accepted for publication 14 June 2006

Introduction

Oculocutaneous albinism (OCA) is a group of autosomal recessive hypopigmentary disorders of the skin, hair and eyes. Mutations in four genes have been reported in different types of human OCA since our first report on OCA1 (Tomita et al., 1989). One of the four OCA types, OCA4, is caused by mutations in the membrane-associated transporter protein gene (*SLC45A2, MATP*) (Newton et al., 2001). The human SLC45A2 protein is a 530-amino-acid polypeptide that contains 12 putative transmembrane domains, and is only expressed in melanocytes (Fukamachi et al., 2001; Harada et al., 2001). Tyrosinase processing and trafficking are disrupted before delivery to early melanosomes in melanocyte cultures established from a mouse model of OCA4 (Costin et al., 2003). The *SLC45A2* gene seems to be transcriptionally modulated by microphthalmia-associated transcription factor (MITF), which is a melanocyte-specific transcription factor, by an indirect mechanism (Du and Fisher, 2002). Clinical phenotypes of OCA4 vary from complete absence to some pigmentation with brown hair and irides, and some patients show improvement during the first decade of life (Inagaki et al., 2004; Rundshagen et al., 2004). Eighteen different mutations in Turkish, German, Korean and Japanese patients with OCA4 have been reported so far (Inagaki et al., 2004, 2005; Newton et al., 2001; Rundshagen et al., 2004; Suzuki et al., 2005).

In this study, we report six novel mutations of the *SLC45A2* gene of eight Japanese patients who showed various clinical phenotypes.

Results

All of the eight patients were Japanese, and their clinical phenotypes and mutations are summarized in Table 1. Patient 1 showed the mildest phenotype among the eight patients (Figure 1A). He had brown hair since infancy, slightly creamy skin with the ability to develop a slight tan, and a pigmented nevus. Visual acuity was 20/30 (right) and 20/20 (left). Patient 8 showed the most severe phenotype (Figure 1B), similar to tyrosinase-negative OCA (OCA1A), which is characterized by the complete absence of pigmentation throughout life. His younger sister showed the

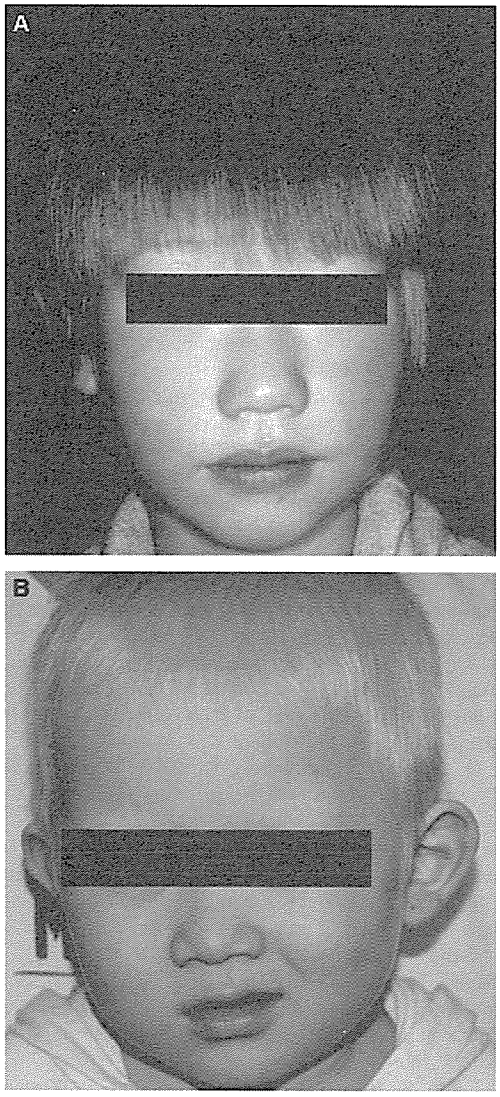

Figure 1. The diverse clinical phenotypes of patients with OCA4. (A) Patient 1, with p.D157N and p.T440A mutations, had brown hair and red-brown irides without nystagmus. (B) Patient 8, with p.G89R and p.G188V mutations, had white hair and blue irides with nystagmus. Note the milder hypopigmentation of patient 1 compared with that of patient 8.

same severe hypopigmentation with white hair, blue eyes and nystagmus.

Six novel mutations, p.Y49C (c.146A > G), p.G89R (c.265G > A), p.C229Y (c.686G > A), p.T437A (c.1309A > G), p.T440A (c.1318A > G), p.G473D (c.1418G > A), and two known mutations, p.D157N (c.469G > A), p.G188V (c.563G > T), were found in the eight patients. These missense substitutions were not detected in 104 control Japanese individuals. Furthermore, all of the missense substitutions were found at amino acid residues conserved between mouse and human. These indicated that all of the missense substitutions could be considered to be pathologic rather than common polymorphisms.

Discussion

The severe phenotype was only observed in patient 8 with the novel p.G89R and reported p.G188V mutations whose hair was white and irides were blue (Figure 1B), suggesting that the p.G89R allele might have no activity in melanogenesis. Further analysis such as a functional assay of the mutant allele in vitro will be needed to confirm the activity, because some examples of a wide variation in pigmentation among OCA patients with the same mutant alleles have been reported in the literature.

So far, a total of 24 different mutations in the *SLC45A2* gene have been reported (Figure 2) (Inagaki et al., 2004, 2005; Newton et al., 2001; Rundshagen et al., 2004; Suzuki et al., 2005). All of the 16 missense mutations were located within or very close to the transmembrane domains, indicating that these areas should be critical for the function of the SLC45A2 protein. Similarly, all of the missense mutations detected in animal models of OCA4 are located within the transmembrane domains of the homologue protein. For example, the missense mutation p.D153N found in the cream coat color horse is within the fourth transmembrane domain (Mariat et al., 2003). In the mouse, UW^{Dbr} (p.D153N) and UW^{d} (p.S435P) have been repor-

Table 1. Mutations of the *SLC45A2* gene in eight patients with OCA4 and their phenotypes

			Mutations		Clinical phenotype		
Patient number	Age	Sex	Maternal	Paternal	Hair color	Iris color	Nystagmus
1	6 years	M	p.D157N	**p.T440A**	Brown	Red-brown	Negative
2	5 months	M	p.G188V	**p.T440A**	Brown	Hazel	Negative
3	8 months	F	**p.T440A**	**p.G89R**	Blond	Brown	Negative
4	11 months	F	**p.T437A**	p.D157N	Blond	Hazel	Negative
5	3 months	M	**p.G473D**	p.D157N	Light brown	Blue	Positive
6	1 year	M	**p.Y49C**[a]	p.D157N[a]	Blond	Blue	Positive
7	4 years	F	**p.C229Y**	p.D157N	Blond	Gray	Positive
8	2 years	M	**p.G89R**	p.G188V	White	Blue	Positive

Novel mutations are in bold.
[a]Maternal and paternal origins were not determined.

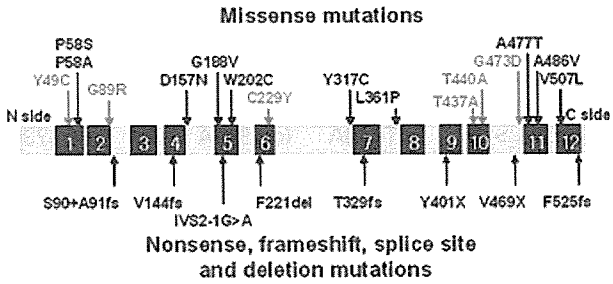

Figure 2. Mutations in the *SLC45A2* gene. Twelve transmembrane domains are boxed with numbers. The mutations reported in this report are shown in red characters. The numbers of the first and last amino acids at the 12 transmembrane domains are 37–65, 69–89, 107–131, 137–155, 184–205, 218–235, 323–347, 366–388, 399–418, 423–441, 476–496 and 503–526, respectively.

ted to be within the fourth and 10th transmembrane domains, respectively (Du and Fisher, 2002; Newton et al., 2001). In medaka fish, four mutations, b^{g21}, b^{d4}, b^{d2}, and b^{d8}, are located within the eighth, ninth, ninth and 10th transmembrane domains, respectively (Fukamachi et al., 2001).

In conclusion, we identified six novel mutations of the *SLC45A2* gene in eight patients with various phenotypes which were speculated to depend on the mutation sites. All of the locations of the missense substitutions were within or very close to the transmembrane domains of the SLC45A2 protein.

Methods

Mutation analysis of the *SLC45A2* gene

Genomic DNA samples were extracted from peripheral blood leukocytes of the patients and their parents. None of the patients was related. All of the seven exons and flanking intron sequences of the *SLC45A2* gene were amplified by polymerase chain reaction (PCR) as described (Inagaki et al., 2004). The amplified PCR products were direct-sequenced to identify any mutations. We also confirmed the mutations with the single strand conformation polymorphism (SSCP) heteroduplex method (Suzuki et al., 2004). The ethics committee of the Nagoya University Graduate School of Medicine approved this study. This study was conducted according to Declaration of Helsinki Principles. Informed consent was obtained from each patient, or from the patient's parents in the case of children.

Acknowledgements

We are grateful to the patients, their families and volunteers for providing blood samples. This work was supported by grant 16591095, 18390312, and 16390315 from Ministry of Education, Science and Culture of Japan, and partially by The Cosmetology Research Foundation.

References

Costin, G.E., Valencia, J.C., Vieira, W.D., Lamoreux, M.L., and Hearing, V.J. (2003). Tyrosinase processing and intracellular trafficking is disrupted in mouse primary melanocytes carrying the underwhite (uw) mutation. A model for oculocutaneous albinism (OCA) type 4. J. Cell. Sci. *116*, 3203–3212.

Du, J., and Fisher, D.E. (2002). Identification of Aim-1 as the underwhite mouse mutant and its transcriptional regulation by MITF. J. Biol. Chem. *277*, 402–406.

Fukamachi, S., Shimada, A., and Shima, A. (2001). Mutations in the gene encoding B, a novel transporter protein, reduce melanin content in medaka. Nat. Genet. *28*, 381–385.

Harada, M., Li, Y.F., El-Gamil, M., Rosenberg, S.A., and Robbins, P.F. (2001). Use of an in vitro immunoselected tumor line to identify shared melanoma antigens recognized by HLA-A*0201-restricted T cells. Cancer Res. *61*, 1089–1094.

Inagaki, K., Suzuki, T., and Shimizu, H. et al. (2004). Oculocutaneous albinism type 4 is one of the most common types of albinism in Japan. Am. J. Hum. Genet. *74*, 466–471.

Inagaki, K., Suzuki, T., Ito, S., Suzuki, N., Fukai, K., Horiuchi, T., Tanaka, T., Manabe, E., and Tomita, Y. (2005). OCA4: Evidence for a founder effect for the p.D157N mutation of the *MATP* gene in Japanese and Korean. Pigment. Cell. Res. *18*, 385–388.

Mariat, D., Taourit, S., and Guerin, G. (2003). A mutation in the MATP gene causes the cream coat colour in the horse. Genet. Sel. Evol. *35*, 119–133.

Newton, J.M., Cohen-Barak, O., Hagiwara, N., Gardner, J.M., Davisson, M.T., King, R.A., and Brilliant, M.H. (2001). Mutations in the human orthologue of the mouse underwhite gene (*uw*) underlie a new form of oculocutaneous albinism, OCA4. Am. J. Hum. Genet. *69*, 981–988.

Rundshagen, U., Zuhlke, C., Opitz, S., Schwinger, E., and Kasmann-Kellner, B. (2004). Mutations in the MATP gene in five German patients affected by oculocutaneous albinism type 4. Hum. Mutat. *23*, 106–110.

Suzuki, T., Ito, S., Inagaki, K., Suzuki, N., Tomita, Y., Yoshino, M., and Hashimoto, T. (2004). Investigation on the IVS5 +5G → A splice site mutation of HPS1 gene found in Japanese patients with Hermansky-Pudlak Syndrome. J. Dermatol. Sci. *36*, 106–108.

Suzuki, T., Inagaki, K., Fukai, K., Obana, A., Lee, S-T., and Tomita, Y. (2005). A Korean case of oculocutaneous albinism type IV caused by a D157N mutation in the *MATP* gene. Br. J. Dermatol. *152*, 174–175.

Tomita, Y., Takeda, A., Okinaga, S., Tagami, H., and Shibahara, S. (1989). Human oculocutaneous albinism caused by single base insertion in the tyrosinase gene. Biochem. Biophys. Res. Commun. *164*, 990–996.

Highlighted paper selected by Editor-in-chief

DNA Damage Caused by Bisphenol A and Estradiol through Estrogenic Activity

Takako Iso,[a,b] Takahide Watanabe,[a,b] Teruaki Iwamoto,[b,c] Akira Shimamoto,[a] and Yasuhiro Furuichi*,[a,b]

[a] *GeneCare Research Institute Co., Ltd.: 200 Kajiwara, Kamakura, Kanagawa 247–0063, Japan:* [b] *Core Research for Evolution Science and Technology, Japan Science and Technology Agency; Kawaguchi Center Building, 4–1–8 Honcho, Kawaguchi, Saitama 332–0012, Japan: and* [c] *Department of Urology, St Marianna University School of Medicine; 2–16–1 Sugao, Miyamae, Kawasaki 216–8511, Japan.* Received September 15, 2005; accepted November 15, 2005

Evidence exists that raises concern about genotoxic effects induced by estrogen: oxidative stress caused by estrogen-derived oxidants, DNA adducts formed by estrogen metabolites and estrogen-induced chromosomal aberration. Estrogen receptors (ER) participate in some of these genotoxic effects by estrogen. In this study, we showed the effects of bisphenol A (BPA), an endocrine-disrupting chemical eliciting weak estrogenic activity, and of 17β-estradiol (E2), on DNA damage in ER-positive MCF-7 cells by Comet assay. Higher concentrations of BPA, more than 1000 times of E2, were needed to induce the same levels of effects by E2. Immunofluorescence microscopy showed that γH2AX, an early marker of DNA breaks, increased after treatment with E2 or BPA in MCF-7 cells. γH2AX foci colocalized with Bloom helicase, which is considered to be responsible for the repair of DNA damage after treatment with E2 or BPA. Interestingly, DNA damage was not as severe in ER-negative MDA-MB-231 cells as in MCF-7 cells. The ER antagonist ICI182780 blocked E2 and BPA genotoxic effects on MCF-7 cells. These results together suggest that BPA causes genotoxicity ER dependently in the same way as E2.

Key words bisphenol A; 17β-estradiol; endocrine-disrupting chemical; DNA damage; Bloom helicase

Epidemiological studies and animal experiments have shown carcinogenic properties of estrogen. Studies to clarify the molecular mechanisms of carcinogenesis by estrogen suggest that estrogen causes carcinogenic effects by combined genotoxicity and stimulation of cell proliferation.[1—3] Estrogen causes DNA damage by estrogen-derived oxidants,[4,5] DNA adducts formed by estrogen metabolites[5,6] and formation of micronuclei.[7,8] Recent studies strongly suggest that DNA damage induced by estrogen is dependent on estrogen receptors (ER): the ER antagonist tamoxifen inhibits E2 effects in ER-positive MCF-7 cells, but not in ER-negative MDA-MB-231 cells.[4,9] Detoxifying enzyme activity markedly decreases by treatment with 17β-estradiol (E2) in MCF-7 cells, leading to increased susceptibility of cells to DNA damage, but E2 has no effect on detoxifying enzyme activity in MDA-MB-231 cells.[4]

Bisphenol A (BPA) was first shown to be estrogenic in 1938 in ovariectomized rats[10] and later in MCF-7 human breast cancer cell culture assay.[11] BPA is an endocrine-disrupting chemical and has a weak affinity for ER, estimated at about 1/1000 of E2,[12] and its additional estrogenic effects on the hormonal homeostatic system has recently received much attention.

We also studied proteins involved in the repair of DNA damage induced by E2 and BPA. Histone H2AX (H2AFX) is responsible for maintaining genomic stability by recognizing DNA double-strand breaks.[13] At the sites of stalled replication forks, H2AX is phosphorylated to γH2AX, which forms foci[14] that appear immediately after DNA damage and recruit proteins responsible for repair of DNA damage, including Bloom helicase (BLM),[14,15] the product of BLM that is the causative gene of Bloom syndrome, an autosomal recessive genetic disorder.[16,17] Clinical features of patients having Bloom syndrome include growth retardation, immunodeficiency, male infertility but not female infertility, and a high incidence of cancers. Cells from Bloom syndrome patients show a high frequency of sister chromatid exchange.[18,19] BLM responds to DNA damage and accumulates at the site of DNA double-strand breaks and physically interacts with γH2AX.[15] In this study we investigated the effects of E2 and BPA on DNA damage in ER-positive MCF-7 and ER-negative MDA-MB-231 cells, both of which are derived from adenocarcinomas; these effects were assessed by alkaline single cell electrophoresis (Comet assay). We also investigated colocalization of γH2AX and BLM at sites of DNA damage.

MATERIALS AND METHODS

Chemicals E2 and BPA were purchased from Wako Pure Chemicals Industries, Ltd. (Osaka). Estrogen receptor antagonist ICI182780 was obtained from TOCRIS (Ellisville, MO, U.S.A.).

Cells, Cell Culture and Chemical Treatment MCF-7 cells and MDA-MB-231 cells were obtained from the American Type Cell Culture (Bethesda, MA, U.S.A.). Cells were maintained in Dulbecco's Modified Eagle's Medium (DMEM) supplemented with 10% fetal bovine serum (FBS) and 50 μg/ml gentamycin (both from Sigma-Aldrich, St. Louis, MO, U.S.A.) in a humidified atmosphere under 5% CO_2 at 37 °C. For all experiments cells were transferred to phenol red-free DMEM supplemented with 10% charcoal-dextran-stripped FBS (Hyclone, Logan, UT, U.S.A.) for 48 h before use to avoid hormonal effects, including by estrogen in FBS. Chemical treatments continued for 1, 3 or 24 h at the indicated concentrations. Pre-treatment with ICI182780 was done for 1 h and then by E2 or BPA treatments. Chemicals were solubilized in ethanol and the final concentration of ethanol in the culture was 0.1%. A control culture was exposed to a culture medium containing 0.1% ethanol.

Colorimetric Assay of Cell Number by WST-8 Method The WST-8 (2-(2-methoxy-4-nitrophenyl)-3-(4-nitrophenyl)-5-(2,4-disulfophenyl)-2*H*-tetrazolium, monosodium salt)

* To whom correspondence should be addressed. e-mail: furuichi@genecare.co.jp

method was used for assessment of cell number. According to the manufacturer's protocol (Nacalai Tesque, Kyoto), WST-8 solution was added to the culture, and then cells were incubated for another 4 h. The absorbance was measured at 450 nm by using a spectrophotometer (ARVO MX, PerkinElmer, Boston, MA, U.S.A.) with a reference wavelengh of 620 nm.

Comet Assay To detect DNA double-strand breaks in a single cell by using Comet assay, alkaline lysis and then alkaline gel electrophoresis were used.[20] Briefly, cells were incubated with various concentrations of E2 or BPA up to 24 h. The cells were treated with trypsin to detach cells from the dish and from each other, and then they were suspended in phosphate-buffered saline (PBS) and were mixed with a 10-fold volume of 1% low-melting-point agarose (FMC Bioproducts, Rockland, ME, U.S.A.). Aliquots (75 μl) of the cell suspension were layered on a fully frosted glass slide (Matsunami, Osaka) pre-coated with 1% agarose. The gel was covered with a cover slip and was incubated at 4 °C for 20 min. The cover slips were removed and the slides were immersed in a lysis solution containing 2.5 M NaCl, 100 mM ethylenediamine-*N*,*N*,*N*′,*N*′-tetraacetic acid (EDTA) at pH 10, 10 mM Tris, 1% lauryl sarcosinate and 1% Triton X-100 for 1 h at 4 °C. The slides were transferred to an alkali solution (300 mM NaOH, 1 mM EDTA, pH >13) at 4 °C for an additional 25 min, and then electrophoresis was done in the fresh alkali electrophoresis solution (300 mM NaOH, 1 mM EDTA, pH >13) at 20 V for 25 min at 4 °C. The cells were neutralized with 400 mM Tris–HCl at pH 7.5 and were fixed in 70% ethanol for 10 min at room temperature. The gel was dried, and the DNA was stained with SYBR Green (Trevigrn, Gaitherburg, MD, U.S.A.). All processes were done under dimmed light to avoid damage by UV. Comet formation of cells was observed at ×400 magnification by using a fluorescence microscopy (Fluoview, Olympus, Tokyo) and the Comet tail length (CTL) was measured for 30 cells (10 cells from each of three slides). Statistical analysis of the CTL values between treated and control groups was done by using Dunnett's test.

Immunofluorescence Microscopy Subnuclear localization of γH2AX and BLM proteins was investigated by using confocal immunofluorescence microscopy (Fluoview, Olympus, Tokyo). Cells were grown to subconfluence on a chamber slide (BD Falcon, Bedford, MA, U.S.A.) in the presence or absence of E2 or BPA. They were fixed with 4% formaldehyde for 10 min at room temperature and were washed three times with PBS containing 0.05% Tween 20. The cells were permeabilized with 0.1% Triton X-100 in PBS for 5 min, and then were blocked with 3% skim milk in PBS for 30 min at room temperature. The following primary antibodies were used: mouse anti-γH2AX monoclonal antibody (Upstate, Charlottesville, VA, U.S.A.) and rabbit anti-BLM polyclonal antibody (Abcam, Cambridge, U.K.). Anti-mouse IgG labeled with Alexa Fluor 594 and anti-rabbit IgG labeled with Alexa Fluor 488 (both from Molecular Probes, Eugene, OR) were used as secondary antibodies. Cells were mounted under cover slips on glass slides in DAKO fluorescent mounting medium (DAKO, Glostrup, Denmark). The detailed procedure was described previously.[21]

RESULTS

Genotoxic Effect of E2 and BPA DNA damage in MCF-7 cells was assessed by measuring the CTL. E2 was added at concentrations from 10^{-9} to 10^{-7} M, which induced Comet formation after 3 h, after which the CTL increased dose dependently (Table 1). Because physiological concentrations of E2 in the blood are between pg/ml and ng/ml (10^{-10} to 10^{-8} M),[22] the significant effective dose of E2 that induced Comet formation is assumed to be within physiological concentrations. A similar effect to induce Comet formation was observed with BPA, but the concentrations needed to induce similar levels of CTL were much higher (Table 1). BPA is generally used in the manufacture of polycarbonate, and elicits weak estrogenic activity[23]: the activity of BPA at concentration 10^{-6} M is almost equivalent to the activity of E2 at concentration 10^{-8} M.[11,24] Thus, the observation of the effective concentrations of BPA (10^{-6} to 10^{-4} M) is consistent with the difference in ER affinity previously reported.[11,24] Notably, effective concentrations of BPA that induce genotoxicity did not affect the viability of MCF-7 cells, indicating that genotoxicity was not due to cytotoxicity of BPA. Figure 1 shows typical Comet formations elicited by E2 and BPA. MCF-7 cells without treatment did not show Comet tail. The Comet assay was done at 1, 3 and 24 h after treatment with 10^{-7} M E2 or 10^{-4} M BPA, and a significant increase in CTL was detectable at 3 h after treatment with E2 and at 1 h after treatment with BPA (Table 2). The increased levels of CTL by treatment with E2 or BPA were remained after the 24-h treatment (Table 2). However, the ER-negative MDA-MB-231 cells were less sensitive to DNA damage by E2 or BPA: 10^{-7} M E2 slightly increased CTL in MDA-MB-231 cells at 3 h, but did not affect CTL at 24 h after treatment (Table 3), nor at ten times higher concentration of E2 at 24 h after treatment (data not shown). BPA at concentration 10^{-4} M slightly increased CTL in MDA-MB-231 cells at 3 and 24 h after treatment, but its effect was much weaker compared with MCF-7 cells (Table 2). These results indicate that ER-positive MCF-7 cells have much higher susceptibility than ER-negative MDA-MB-231 cells and support the idea that ER participates in genotoxicity by E2 or BPA.

Further Evidence of ER Participation in Genotoxicity by E2 or BPA To investigate further if ER participate in DNA damage by E2 or BPA, the effect of ER antagonist ICI182780 on the effect of E2 or BPA to induce genotoxicity was studied. MCF-7 cells were pre-treated with 10^{-6} M

Table 1. Effect of E2 and BPA on Comet Formation in MCF-7 Cells after 3 h Treatment

Treatment	Concentration (M)	Cell number (%)[a]	Comet tail length (μm)[b]
Control (0.1% ethanol)		100	12.80±2.00
E2	10^{-11}	105	15.15±3.76
	10^{-9}	103	22.61±9.89**
	10^{-7}	101	28.21±9.70**
Control (0.1% ethanol)		100	11.54±2.78
BPA	10^{-8}	104	15.94±6.95
	10^{-6}	93	20.73±8.16**
	10^{-4}	96	29.47±11.69**

a) Percentage of control as assessed by WST-8 assay. *b*) Mean±S.D., 30 cells. ** $p<0.01$.

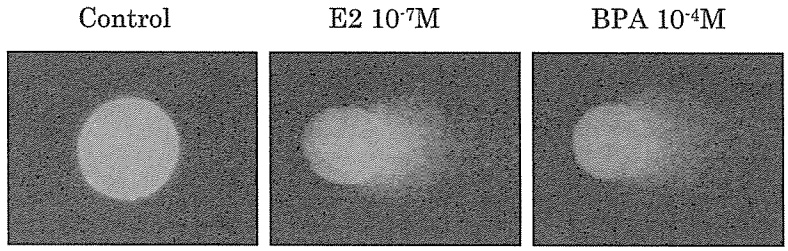

Fig. 1. Comet Formation Induced by E2 and BPA

MCF-7 cells treated with 10^{-7} M E2 or 10^{-4} M BPA for 3 h show typical tails.

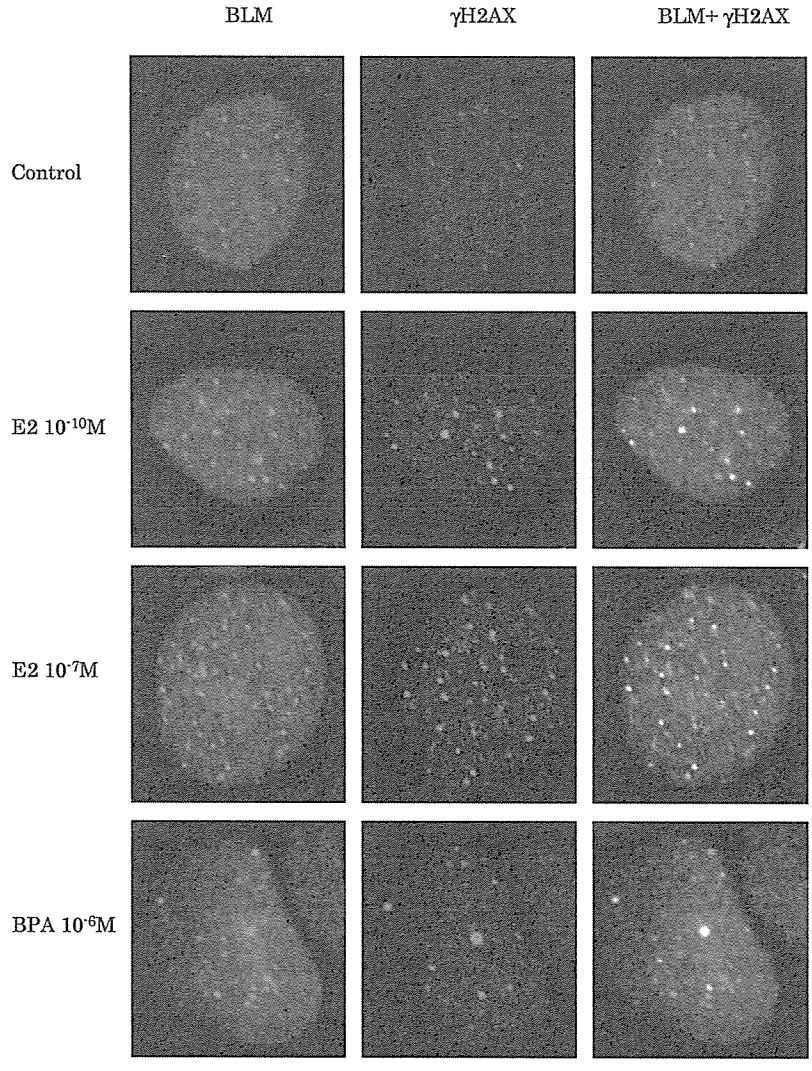

Fig. 2. Localization of BLM with γH2AX after DNA Damage Induced by E2 and BPA

MCF-7 cells treated with 10^{-10} and 10^{-7} M E2 or 10^{-6} M BPA for 3 h, were simultaneously stained with anti-BLM and anti-γH2AX antibodies. BLM and γH2AX were stained green and red, respectively. Colocalization of BLM and γH2AX were stained yellow.

ICI182780 for 1 h and then were treated with 10^{-7} M E2 or 10^{-6} and 10^{-4} M BPA for 3 h. The pre-treatment with ICI182780 antagonized the genotoxic effect by E2 or BPA, and an increase in CTL by E2 or BPA was not observed in the presence of ICI182780 (Table 4). These results also strongly support the idea that ER participate in the genotoxic effect by E2 or BPA.

Replication Stress after Treatment with E2 or BPA

Histone H2AX has been implicated in the maintenance of genomic stability by participating in the repair of DNA damage.[14,15] H2AX is phosphorylated to γH2AX, which then forms foci in response to DNA double-strand breaks resulting in replication arrest in cells.[13] γH2AX foci are formed rapidly in response to DNA damage.[14] In this study, 10—20 γH2AX foci appeared in the MCF-7 nucleus at 3 h after treatment with E2 or BPA (Fig. 2). Fluorescence signals of

Table 2. Time-Course Analysis of DNA Damage Induced by E2 and BPA in MCF-7 Cells

Treatment	Concentration (M)	1 h		3 h		24 h	
		Cell number (%)[a]	Comet tail length (μm)[b]	Cell number (%)[a]	Comet tail length (μm)[b]	Cell number (%)[a]	Comet tail length (μm)[b]
Control (0.1% ethanol)		100	14.70±7.32	100	11.30±2.95	100	12.99±2.33
E2	10^{-7}	100	17.69±6.60	101	41.79±14.40**	106	37.33±12.87**
BPA	10^{-4}	97	29.77±34.46*	96	37.67±11.31**	109	43.91±19.16**

a) Percentage of control as assessed by WST-8 assay. *b*) Mean±S.D., 30 cells. * $p<0.05$, ** $p<0.01$.

Table 3. Effect of E2 and BPA on Comet Formation in ER-Negative MDA-MB-231 Cells

Treatment	Concentration (M)	3 h		24 h	
		Cell number (%)[a]	Comet tail length (μm)[b]	Cell number (%)[a]	Comet tail length (μm)[b]
Control (0.1% ethanol)		100	7.03±2.49	100	9.15±2.15
E2	10^{-7}	99	9.34±2.44*	92	9.99±2.26
BPA	10^{-4}	96	8.97±3.69*	94	10.63±2.22*

a) Percentage of control as assessed by WST-8 assay. *b*) Mean±S.D., 30 cells. * $p<0.05$.

Table 4. DNA Damage Induced by E2 and BPA in the Presence of ICI182780 in MCF-7 Cells

Treatment	Concentration (M)	Cell number (%)[a]	Comet tail length (μm)[b]
Control (0.1% ethanol)		100	3.26±3.10
E2	10^{-7}	101	25.77±12.84**
ICI	10^{-6}	100	6.21±2.39
ICI/E2	$10^{-6}/10^{-7}$	90	6.52±2.51
Control (0.1% ethanol)		100	9.48±2.51
BPA	10^{-6}	101	26.41±6.62**
ICI	10^{-6}	96	10.33±2.57
ICI/BPA	$10^{-6}/10^{-6}$	102	11.13±3.19
Control (0.1% ethanol)		100	11.12±3.31
BPA	10^{-4}	96	27.42±6.74**
ICI	10^{-6}	90	12.83±4.66
ICI/BPA	$10^{-6}/10^{-4}$	92	11.46±5.58

a) Percentage of control as assessed by WST-8 assay. *b*) Mean±S.D., 30 cells. ICI/E2: pre-treatment with ICI182780 followed by E2 treatment. ICI/BPA: pre-treatment with ICI182780 followed by BPA treatment. ** $p<0.01$.

γH2AX foci intensified as the concentration of E2 increased, but the foci remained indistinct in untreated MCF-7 cells. These results are consistent with the results by Comet assay that E2 and BPA induced DNA double-strand breaks. γH2AX foci were indistinct in ER-negative MDA-MB-231 cells treated with E2 or BPA (data not shown). By using anti-BLM antibody BLM partially colocalized with γH2AX foci, suggesting that part of BLM was associated with damaged DNA sites. BPA treatment produced a similar result. Notably, large foci colocalized with BLM and γH2AX, which were shown by yellow staining and were obvious in cells treated with E2 or BPA but not in untreated control cells. These results suggest that DNA double-strand breaks caused by E2 or BPA stimulate formation of γH2AX foci and accumulate BLM in the foci.

DISCUSSION

Although genotoxic effects of E2 are ER-dependent, the sensitivity of ER-negative cells to E2 effects is inconsistent: E2 metabolites are genotoxic in ER-negative MDA-MB-231 cells[5] and physiological doses of E2 induce oxidative DNA damage in MDA-MB-231 cells.[9] However, E2 induces micronuclei formation in ER-positive tumor cells from breast and ovary, but not in ER-negative cells.[8,25] In this study, we showed: 1) E2 or BPA produced statistically significant genotoxic effects in ER-positive MCF-7 cells, but much less genotoxic effects, if any, in MDA-MB-231 cells, 2) ER antagonist ICI182780 weakened E2 and BPA genotoxic effects in MCF-7 cells and 3) E2 stimulated formation of γH2AX foci colocalized with BLM. These results strongly support the idea that genotoxic effects of E2 are mediated by ER. Our results and conclusion are supported by the evidence that estrogen-induced DNA damage is inhibited by the estrogen receptor antagonist tamoxifen.[8,9,25] Also, E2 downregulates detoxifying enzyme activity ER dependently.[4] And, Fischer *et al.*[8] and Stopper *et al.*[25] suggest DNA damage may be due to an overriding checkpoint under ER-dependent cell proliferation induced by hormone.

We conclusively showed, we believe for the first time, that BPA had essentially similar effects as E2 to cause DNA damage depending on ER in MCF-7 cells, although higher concentrations of BPA were needed. Lee *et al.*[26] observed genotoxicity of BPA by using Comet assay in mouse lymphoma cells, but they concluded that the effect was false positive due to cell death, because effective doses of 4×10^{-6}—4×10^{-4} M BPA were cytotoxic. In our study, BPA at doses of 10^{-6}—10^{-4} M were genotoxic in MCF-7 cells but were not cytotoxic, excluding the possibility that genotoxicity was due to cytotoxicity. Interestingly, BPA administration reduces the activity of detoxifying enzymes, including superoxide dismutase, glutathine peroxidase and catalase, in mouse tissue,[27] consistent with E2 markedly suppressing enzymes to metabolize oxidative products in MCF-7 cells.[4] To cause DNA damage, BPA, an endocrine-disrupting chemical, needed higher concentrations than the levels of BPA detected in various kinds of human biological fluids contaminated with this compound.[28] Studies of the biological fate of BPA by using animal tests have shown that most radioactivity is

recovered in urine and feces at about 7 d after administration of ^{14}C- BPA in rats.[29—31] These observations suggest BPA is not likely to accumulate in the body. Overall, genotoxicity of BPA may not be serious.

H2AX is rapidly phosphorylated to γH2AX, which forms foci at the sites of DNA double-strand breaks. BLM at γH2AX sites and is considered to interact with the DNA damage response protein 53BP1 and to participate in DNA repair processes.[15] Our preliminary study (Iso *et al.*, unpublished data) showed that damage induced by E2 and BPA was restored reversibly in MCF-7 cells: when cells were cultured for 24 h in the absence of E2 or BPA after 24 h-treatment of cells with E2 or BPA, few Comet forming cells were observed. Thus, the integrity of DNA structure may be recovered, probably by a system to stabilize the genome, including DNA repair enzymes such as BLM.

To sum up, our findings contribute to show genotoxicity of estrogenic agents, including BPA, ER dependently, and whether genomic instability induced by estrogenic agents can be overcome in a DNA repair system will be of further interest.

Acknowledgements We thank Dr. Masanobu Sugimoto, GeneCare Research Institute, for his discussion and help in reviewing this manuscript. This study was supported by the Japan Science and Technology Agency, Japan.

REFERENCES

1) Bhat H. K., Calaf G., Hei T. K., Loya T., Vadgama J. V., *Proc. Natl. Acad. Sci. U.S.A.*, **100**, 3913—3918 (2003).
2) Liehr J. G., *Endocr. Rev.*, **21**, 40—54 (2000).
3) Cavalieri E., Frenkel K., Liehr J. G., Rogan E., Roy D., *J. Natl. Cancer Inst. Monogr.*, **27**, 75—93 (2000).
4) Mobley J. A., Brueggemeier R. W., *Carcinogenesis*, **25**, 3—9 (2004).
5) Chen Y., Liu X., Pisha E., Constantinou A. I., Hua Y., Shen L., van Breemen R. B., Elguindi E. C., Blond S. Y., Zhang F., Bolton J. L., *Chem. Res. Toxicol.*, **13**, 342—350 (2000).
6) Cavalieri E. L., Li K.-M., Balu N., Saeed M., Devanesan P., Higginbotham S., Zhao J., Gross M. L., Rogan E. G., *Carcinogenesis*, **23**, 1071—1077 (2002).
7) Yared E., McMillan T. J., Martin F. L., *Mutagenesis*, **17**, 345—352 (2002).
8) Fischer W. H., Keiwan A., Schmitt E., Stopper H., *Mutagenesis*, **16**, 209—212 (2001).
9) Bianco N. R., Perry G., Smith M. A., Templeton D. J., Montano M. M., *Mol. Endocrinol.*, **17**, 1344—1355 (2003).
10) Dodds E. C., Lawson W., *Proc. R. Soc. Biol.*, **125**, 222—232 (1938).
11) Krishnan A. V., Stathis P., Permuth S. F., Tokes L., Feldman D., *Endocrinology*, **132**, 2279—2286 (1993).
12) Gould J. C., Leonard L. S., Maness S. C., Wagner B. L., Conner K., Zacharewski T., Safe S., McDonnell D. P., Gaido K. W., *Mol. Cell. Endocrinol.*, **142**, 203—214 (1998).
13) Ward I. M., Chen J., *J. Biol. Chem.*, **276**, 47759—47762 (2001).
14) Davalos A. R., Campisi J., *J. Cell Biol.*, **162**, 1197—1209 (2003).
15) Sengupta S., Robles A. I., Linke S. P., Sinogeeva N. I., Zhang R., Pedeux R., Ward I. M., Celeste A., Nussenzweig A., Chen J., Halazonetis T. D., Harris C. C., *J. Cell Biol.*, **166**, 801—813 (2004).
16) Ellis N. A., Groden J., Ye T.-Z., Straughen J., Lennon D. J., Ciocci S., Proytcheva M., German J., *Cell*, **83**, 655—666 (1995).
17) Karow J. K., Chakraverty R. K., Hickson I. D., *J. Biol. Chem.*, **272**, 30611—30614 (1997).
18) Hickson I. D., Davies S. L., Li J.-L., Levitt N. C., Mohaghegh P., North P. S., Wu L., *Biochem. Soc. Trans.*, **29**, 201—204 (2001).
19) Nicotera T. M., *Cancer Genet. Cytogenet.*, **53**, 1—13 (1991).
20) Miyamae Y., Zaizen K., Ohara K., Mine Y., Sasaki Y. F., *Mutat. Res.*, **415**, 229—235 (1998).
21) Shiratori M., Suzuki T., Itoh C., Goto M., Furuichi Y., Matsumoto T., *Oncogene*, **21**, 2447—2454 (2002).
22) Zeisler H., Jirecek S., Hohlagschwandtner M., Knofler M., Tempfer C., Livingston J. C., *Wien. Klin. Wochenschr.*, **114**, 458—461 (2002).
23) Roy D., Palangat M., Chen C.-W., Thomas R. D., Colerangle J., Atkinson A., Yan Z.-J., *J. Toxicol. Environ. Health*, **50**, 1—29 (1997).
24) Hiroi H., Tsutsumi O., Momoeda M., Takai Y., Osuga Y., Taketani Y., *Endocr. J.*, **46**, 773—778 (1999).
25) Stopper H., Schmitt E., Gregor C., Mueller S. O., Fischer W. H., *Mutagenesis*, **18**, 243—247 (2003).
26) Lee M., Kwon J., Chung M.-K., *Mutat. Res.*, **541**, 9—19 (2003).
27) Kabuto H., Hasuike S., Minagawa N., Shishibori T., *Environ. Res.*, **93**, 31—35 (2003).
28) Ikezuki Y., Tsutsumi O., Takai Y., Kamei Y., Taketani Y., *Hum. Reprod.*, **17**, 2839—2841 (2002).
29) Kurebayashi H., Betsui H., Ohno Y., *Toxicol. Sci.*, **73**, 17—25 (2003).
30) Snyder R. W., Maness S. C., Gaido K. W., Welsch F., Sumner S. C. J., Fennell T. R., *Toxicol. Appl. Pharmacol.*, **168**, 225—234 (2000).
31) Pottenger L. H., Domoradzki J. Y., Markham D. A., Hansen S. C., Cagen S. Z., Waechter Jr. J. M., *Toxicol. Sci.*, **54**, 3—18 (2000).

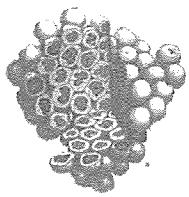

STEM CELLS®

CTACK/CCL27 Accelerates Skin Regeneration via Accumulation of Bone Marrow-Derived Keratinocytes

Daisuke Inokuma, Riichiro Abe, Yasuyuki Fujita, Mikako Sasaki, Akihiko Shibaki, Hideki Nakamura, James R. McMillan, Tadamichi Shimizu and Hiroshi Shimizu

Stem Cells 2006;24;2810-2816; originally published online Aug 24, 2006;
DOI: 10.1634/stemcells.2006-0264

STEM CELLS
TISSUE-SPECIFIC STEM CELLS

CTACK/CCL27 Accelerates Skin Regeneration via Accumulation of Bone Marrow-Derived Keratinocytes

DAISUKE INOKUMA,[a] RIICHIRO ABE,[a] YASUYUKI FUJITA,[a] MIKAKO SASAKI,[a] AKIHIKO SHIBAKI,[a] HIDEKI NAKAMURA,[a] JAMES R. MCMILLAN,[a] TADAMICHI SHIMIZU,[b] HIROSHI SHIMIZU[a]

[a]Department of Dermatology, Hokkaido University Graduate School of Medicine, Sapporo, Japan; [b]Department of Dermatology, Faculty of Medicine, University of Toyama, Toyama, Japan

Key Words. Bone marrow-derived stem cell • CTACK/CCL27 • CCR10 • Keratinocyte • Wound healing

ABSTRACT

Recent studies have suggested that bone marrow (BM) cells transdifferentiate to regenerate a variety of cellular lineages. Due to the relatively small population of BM-derived cells in each organ, it is still controversial whether these BM-derived cells are really present in sufficient numbers for effective function. Conversely, it is speculated that chemokine/chemokine receptor interactions mediate this migration of the tissue-specific precursor cells from BM into the target tissue. Here, we show that cutaneous T-cell attracting chemokine (CTACK)/CCL27 is the major regulator involved in the migration of keratinocyte precursor cells from BM into skin. By screening various chemokine expression patterns, we demonstrated that CTACK is constitutively expressed in normal skin and upregulated in wounds and that approximately 20% of $CD34^+$ BM cells expressed CCR10, the ligand for CTACK. Intradermal injection of CTACK/CCL27 into the periphery of skin wounds significantly enhanced BM-derived keratinocyte (BMDK) migration, and CTACK/CCL27 neutralizing antibody inhibited this BMDK migration. Furthermore, increased BMDK migration caused by CTACK/CCL27 significantly accelerated the wound-healing process without any influence over either angiogenesis or keratinocyte proliferation. These results provide direct evidence that recruitment of BM keratinocyte precursor cells to the skin is regulated by specific chemokine/chemokine receptor interactions, making possible the development of new regenerative therapeutic strategies. STEM CELLS *2006;24:2810–2816*

INTRODUCTION

Bone marrow (BM)-derived stem cells residing in adult BM possess the unique ability to self-renew and differentiate into multiple cell lineages. A number of recent studies have suggested that BM cells might transdifferentiate and contribute to the regeneration of a variety of nonhematopoietic cell lineages in multiple organs [1–3]. Recent studies have shown that epithelial phenotype BM-derived cells can be found in normal and malignant epithelia without evidence of fusion [4–6] and that cutaneous injury leads to increased engraftment of these BM-derived cells as epidermal cells [7].

Thus far, the concept of BM-derived stem cell plasticity has been cautiously accepted; however, several hurdles remain that have blocked the development of clinical applications. The characteristics of BM-derived stem cells are not fully understood (e.g., the mechanisms causing the tissue-specific migration). Tissue repair and regeneration after injury are thought to involve selective recruitment of circulating or resident stem cell populations [8]. BM-derived, transdifferentiated cells have been detected at the wound site in injured tissues; however, the numbers of these cells are so low that it is impossible to confirm any of their specific biological characteristics or functions.

To increase numbers of BM-derived, transdifferentiated cells, two strategies have been employed. One is to increase the number of BM-derived stem cells present in circulating blood (e.g., using granulocyte colony stimulating factor (G-CSF) to induce mobilization of BM cells [9]) and another is to induce tissue-specific recruitment to increase the final number of BM-derived, transdifferentiated cells in the target tissue (e.g., using stromal cell-derived factor-1α [SDF-1α] to induce homing of hematopoietic stem cells to the BM by binding to CXCR4 [10, 11]). Chemokine/chemokine receptor interactions are thus predicted to play important roles in tissue-specific BM-derived stem cell recruitment.

To further our understanding of the chemokine/chemokine receptor interactions involved in tissue-specific stem cell trafficking, we have investigated the mechanism that controls in vivo migration of BM-derived keratinocyte (BMDK) precursor

Correspondence: Hiroshi Shimizu, M.D., Ph.D., Department of Dermatology, Hokkaido University Graduate School of Medicine, N 15 W 7, Kita-ku, Sapporo 060-8638, Japan. Telephone: +81-11-716-1161, ext. 5962; Fax: +81-11-706-7820; e-mail: Shimizu@med.hokudai.ac.jp Received April 30, 2006; accepted for publication August 14, 2006; first published online in STEM CELLS *EXPRESS* August 24, 2006. 1066-5099/2006/$20.00/0 doi: 10.1634/stemcells.2006-0264

cells into the skin. In addition, to elucidate whether BMDKs have any of the functional roles of keratinocytes, we investigated the contribution of BMDKs to the processes involved in wound healing.

Materials and Methods

Generation of BM-Chimeric Mice

Whole BM cells (5×10^6) from green fluorescent protein (GFP)-transgenic (under control of β-actin promoter) mice (The Jackson Laboratory, Bar Harbor, ME, http://www.jax.org) were transplanted into lethally irradiated (8.5 Gy) wild-type C57BL/6 recipients. Hematopoietic reconstitution was subsequently evaluated in peripheral blood 4 weeks after transplantation.

Wounded and Normal Skin Tissue Preparation

All animal procedures were conducted according to guidelines provided by the Hokkaido University Institutional Animal Care and Use Committee under an approved protocol. We performed skin injury and examined for GFP-expressing cells at least 10 weeks after BM transplantation. The mice were anesthetized, and 6-mm full-thickness punch biopsy wounds were made by folding the back skin. The wounded tissues were subsequently collected after 24 hours in reverse transcription-polymerase chain reaction (RT-PCR) analysis and Western blot analysis or after 3 days in immunofluorescence staining.

RT-PCR Analysis

Total RNA was isolated from normal or wounded skin. RT-PCR analyses of mRNA from chemokines and glyceraldehyde-3-phosphate dehydrogenase (GAPDH) were performed in a thermocycler (GeneAmp PCR system 9600; PerkinElmer Life and Analytical Sciences, Boston, http://www.perkinelmer.com). Primers were as follow: cutaneous T-cell attracting chemokine (CTACK) (sense: 5′-AGCAGCCTCCCGCTGTTACTGTTG-3′, antisense: 5′-TGCTTTATTAGTTTTGCTGTTGGG-3′), mucosae-associated epithelial chemokine (sense: 5′-CATACTTCCCATGGCCTCC-3′, antisense: 5′-GAGAGGCTTCGTGCCTGTG-3′), secondary lymphoid tissue chemokine (SLC) (sense: 5′-ATGGCTCAGATGATGACTCT-3′, antisense: 5′-TACTGGGCTATCCTCTTGA-3′), SDF-1α (sense: 5′-AGTGACGGTAAACCAGTCAG-3′, antisense: 5′-CTTTCTCCAGGTACTCTTGG-3′), macrophage inflammatory protein (MIP)-1α (sense: 5′-AAGGTCTCCACCACTGCCCTTG-3′, antisense: 5′-CTCAGGCATTCAGTTCCAGGTC-3′), MIP-1β (sense: 5′-CCAGCTGTGGTATTCCTGACC-3′, antisense: 5′-AATAGCAGAGTTTCAGCAATGG-3′), MIP-2 (sense: 5′-AGTGAACTGCGCTGTCAATG-3′, antisense: 5′-CTTTGGTTCTTCCGTTGAGG-3′), MIP-3α (sense: 5′-CAAGCGTCTGCTCTTCCTTG-3′, antisense: 5′-TGGATCAGCGCACACAGATT-3′), RANTES (sense: 5′-ATAACGCGTATGCATCACCATATGGCTCGGAC-3′, antisense: 5′-CCAGATCTAGCTCATCTCCAAATAG-3′), TARC (thymus and activation-regulated chemokine) (sense: 5′-AGTGGAGTGTTCCAGGGATG-3′, antisense: 5′-TTTGTGTTCGCCTGTAGTGC-3′), monocyte chemoattractant protein (MCP)-2 (sense: 5′-AGTGCTTCTTTGCCTGCTGCTCATAG-3′, antisense: 5′-ATGAGAAAACACGCAGCCCAGGCACC-3′) MCP-5 (sense: 5′-CTATGCCTCCTGCTCATAGC-3′, antisense: 5′-CTTAACCCACTTCTCCTTGG-3′), TECK (thymus-expressed chemokine) (sense: 5′-CTGGGTTACCAGCACAGGAT-3′, antisense: 5′-CCTCTGGATTCCCACACACT-3′), interferon-γ (IFN-γ) inducible protein-10 (sense: 5′-GGGCCAGTGAGAATGAGGGC-3′, antisense: 5′-TGAGCTAGGGAGGACAAGGAG-3′), MIG (monokine induced by IFN-γ) (sense: 5′-GATCAAACCTGCCTAGATCC-3′, antisense: 5′-GGCTGTGTAGAACACAGAGT-3′), and GAPDH (sense: 5′-GAGGGGCCATCCACAGTCTTC-3′, antisense: 5′-CATCACCATCTTCCAGGAGCG-3′). Aliquots from each amplification reaction were analyzed by electrophoresis in 5% acrylamide-Tris-borate gels.

Western Blot Analysis

Protein lysates from normal and wounded skin tissues were electrophoresed on polyacrylamide gels under reducing conditions and then blotted onto nitrocellulose filters. Filters were blocked with nonfat dried milk and followed by incubation with a primary antibody against SDF-1α (Santa Cruz Biotechnology, Inc., Santa Cruz, CA, http://www.scbt.com), SLC, CTACK, MIP-1α, and MIP-1β (R&D Systems, Inc., Minneapolis, http://www.rndsystems.com). After incubation, the filters were treated with horseradish peroxidase-conjugated anti-rabbit immunoglobulin G, and the resultant immune complexes were visualized.

Immunofluorescence Staining

After 28 days, the wounded tissues were removed. Skin sections were stained with primary antibodies to keratin-14 (Chemicon International, Temecula, CA, http://www.chemicon.com), and the chemokines were used in Western blot analysis. Primary antibodies were visualized using secondary antibodies conjugated to fluorescein isothiocyanate (FITC) or rhodamine isothiocyanate. Fluorescence staining was detected using a confocal laser scanning fluorescence microscope (Laser Scanning Confocal Imaging System MRC 1024; Bio-Rad, Hercules, CA, http://www.bio-rad.com). Keratinocytes expressing both keratin-14 and GFP were presumed to be BMDKs. The number of BMDKs was quantified and calculated as a percentage of the total number of keratinocytes in wounded skin.

Chemokine Receptor Expression in $CD34^+$ BM Cells

BM cells were incubated with FITC-conjugated antibody against CD34 (BD Pharmingen, San Diego, http://www.bdbiosciences.com/pharmingen) and antibodies to CXCR4 (BD Pharmingen), CCR7 (Santa Cruz Biotechnology, Inc.), and CCR10 (Calbiochem, San Diego, http://www.emdbiosciences.com) with secondary PE-conjugated antibodies and then analyzed by flow cytometry (FACScalibur; Becton Dickinson Immunocytometry Systems, San Jose, CA, http://www.bdbiosciences.com).

Migration Assays

Migration assays were performed using Costar Transwell (Corning, Acton, MA, http://www.corning.com) inserts (pore size: 3 μm). Isolated $CD34^+$ BM cells purified by fluorescence-activated cell sorting (FACSVantage; BD Biosciences, San Jose, CA, http://www.bdbiosciences.com) based on surface CD34 staining (>99% purity) were suspended at 1×10^6 cells per milliliter in RPMI 1640 medium containing 0.1% fetal bovine serum. Medium alone or medium containing SDF-1α, SLC, or CTACK (R&D Systems, Inc.) at concentrations of 0, 10, 100, or

500 ng/ml was added to individual lower wells of a 24-well plate. $CD34^+$ BM cells were layered on top of the membrane in the upper chamber of the transwell insert and incubated for 18 hours. For checkerboard analysis, chemokines (100 ng/ml) were added to both the bottom and top chambers. Migration was assessed by counting the cell number in the lower wells. Replicate experiments were performed with separate cultures of cells on separate occasions.

Chemokine Intradermal Injection into the Peripheral Wounded Site

BM-chimeric mice were locally anesthetized and given 4-mm, round skin wounds and received a single intradermal injection of SDF-1α, SLC, or CTACK (1 μg in 30 μl) or phosphate-buffered saline (PBS) (as control) into the peripheral wound sites. After 28 days, the wounded tissue was removed, and the percentage of BMDKs in the wounded skin was calculated.

Neutralizing Antibody Injection into the Wounded Skin

CTACK-neutralizing antibody (0–16 μg in 120 μl) was injected into the periphery of the 4-mm, round wound site, and the percentage of BMDKs in the wounded skin was analyzed as described above.

Mobilization of BM Cells

BM cells of BM-chimeric mice were mobilized into peripheral blood by three daily injections of recombinant mouse G-CSF (TECNE, R&D Systems, Inc.) (150 μg/kg per day). Control mice received a sterile saline solution without G-CSF. Twenty-four hours after the last injection, the mice were given epidermal wounds and received intradermal injections of SDF-1α, SLC, or CTACK (1 μg in 30 μl) or PBS (as control) into their peripheral wounds. Twenty-eight days after wounding, the sites were examined to detect BMDKs as described above.

$CD34^+$ BM Cell Adoptive Transfer

$CD34^+$ BM cells from GFP-transgenic mice were purified using the MACS (magnetic cell sorting) technique (Miltenyi Biotec, Bergisch Gladbach, Germany, http://www.miltenyibiotec.com). Immediately after tail vein injection of $CD34^+$ BM cells (5×10^5 cells/mouse), the mice were given skin wounds and received SDF-1α, SLC, or CTACK (1 μg in 30 μl) or PBS (as control) in their peripheral wound sites. After 28 days of wound healing, BMDKs were counted as described above.

Wound-Healing Analysis

Ten-millimeter, round skin wounds were created, and CTACK (total 3 μg in 100 μl), CTACK-neutralizing antibody (total 16 μg in 100 μl), or PBS (100 μl) (as a control) was injected into the peripheral wound sites. Standardized images of wounds were recorded using a digital camera for analysis of daily wound closure rates.

Analysis of Wound-Healing Angiogenesis

BM-chimeric mice were given 4-mm, round skin wounds and received an intradermal injection of CTACK (1 μg in 30 μl) into the periphery of wounds. After 3 days, the wound sites were removed and skin sections were cut and stained with primary antibodies to CD31 (a marker of endothelial cells) (BD Pharmingen) followed by a secondary antibody conjugated to rhodamine isothiocyanate. The number of capillaries in the dermis of the wounded skin was calculated per surface area or volume of tissue.

Proliferation Assay

Keratinocytes were prepared from the skin of a newborn C57BL/6 mouse. After separation of the epidermis from the dermis with dispase and then 0.5% trypsin, the keratinocytes were cultured in 96-well plates at 1,000 cells in 100 μl of keratinocyte growth medium (Cambrex, East Rutherford, NJ, http://www.cambrex.com) per well. After 24 hours of culture, CTACK was added at concentrations of 1–100 ng/ml. After 72 hours of incubation at 37°C, 10 μl of the tetrazolium salt WST-1 (Dojindo Laboratories, Kumamoto, Japan, http://www.dojindo.co.jp) was added to each well [12]. The plates were incubated for 2 hours at 37°C, and viable cells were determined using a microplate reader at 450 nm with a 630 nm reference wavelength.

In Vitro Keratinocyte Migration Assay

Keratinocytes from C57BL6 mice were cultured in six-well uncoated plates with keratinocyte growth medium until they reached 80% confluency. A cell-free area was created by scraping the keratinocyte monolayer with a plastic pipette tip. Keratinocyte migration to the cell-free area was evaluated after 48 hours of culture in medium alone or medium containing CTACK at concentrations of 0, 1, 10, or 100 ng/ml. The number of migrating keratinocytes was counted in four nonoverlapping fields [13].

RESULTS

BMDKs Were Present in the Basal Layer of the Epidermis

We used a GFP transgenic BM transplantation model. The recipient mice had been lethally and completely irradiated, but to enable their long-term survival, BM was reconstituted from the cells of a donor GFP transgenic mouse. Recruitment of BMDKs to the skin was assessed after the induction of full-thickness wounds. Twenty-eight days after the first incision, the wound was excised and examined for BMDK recruitment. Cells expressing both GFP (a marker of BM origin) and keratin-14 (a marker of basal keratinocyte) were present in the basal layer of the epidermis and were classified as BMDKs (Fig. 1A). Some BM-derived cells are likely to be epidermal Langerhans' cells derived from BM, but the GFP^+ keratin-14^+ cells did not express CD45 (a marker of hematopoietic cells) and CD11c (a marker of Langerhans' cells) (data not shown). Almost all BMDKs were present in the basal layer, but some BMDKs were also present in the bulge region of hair follicles. The percentage of BMDKs as a ratio of all keratinocytes was assessed on three sections from one mouse ($n = 5$). BMDKs were calculated to be present as a total of 0.025% $\pm$ 0.009% of all keratinocytes and comprised approximately 0.1% in the basal cell layer.

SDF-1α, SLC, and CTACK Were Expressed in Normal Skin, and CTACK Expression Was Upregulated in Wounded Skin

We therefore supposed that optimum BMDK migration required a higher level of cell recruitment signal generation, such as after

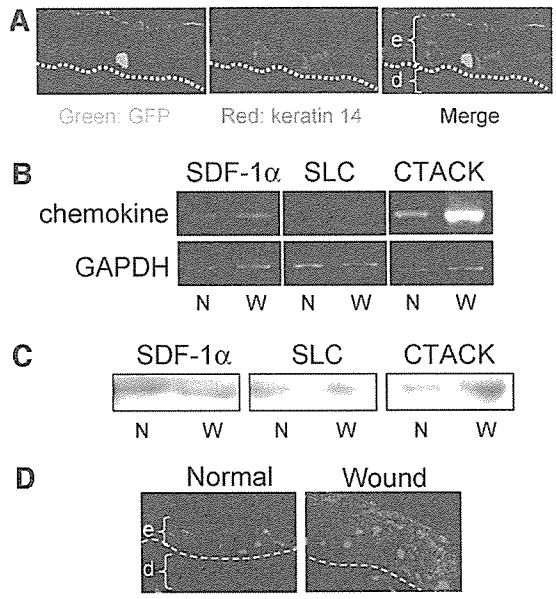

Figure 1. Bone marrow-derived keratinocytes (BMDKs) were identified and CTACK was expressed in wounded skin. **(A):** Engrafted BMDKs in wounded skin expressed both GFP, as a marker of bone marrow origin (green), and keratin-14, as a marker of basal keratinocyte (red), (arrows). **(B–D):** Normal (N) or wounded (W) skin tissue samples were collected and analyzed for chemokine expression as shown in Table 1. The expressions of SDF-1α, SLC, and CTACK were detected by RT-PCR **(B)** and Western blot analysis **(C)** in normal skin and also in skin 24 hours after wounding. These experiments of RT-PCR and Western blot analyses were performed in triplicate. In immunofluorescence staining in the wound edge 3 days after wounding, CTACK expression, in particular, was upregulated (green) **(D)**. SDF-1α and SLC were weakly expressed (data not shown). Nuclei were counterstained with propidium iodide (red). Abbreviations: CTACK, cutaneous T-cell attracting chemokine; d, dermis; e, epidermis; GAPDH, glyceraldehyde-3-phosphate dehydrogenase; GFP, green fluorescent protein; RT-PCR, reverse transcription-polymerase chain reaction; SDF-1α, stromal cell-derived factor-1α; SLC, secondary lymphoid tissue chemokine.

Table 1. Chemokine expression in normal and wounded skin

	RT-PCR		Western blot		IFS	
Wound	**N**	**W**	**N**	**W**	**N**	**W**
SDF	+	+	+	+	+	−
SLC	+	−	+	+	+	−
CTACK	+	+	+	+	+	+
MIP-1α	−	+	−	−	−	−
MIP-1β	−	+	−	−	−	−

MEC (mucosae-associated epithelial chemokine), MIP-2, MIP-3α, RANTES, TARC (thymus and activation regulated chemokine), MCP-2, MCP-5, TECK (thymus-expressed chemokine), IP-10, and MIG (monokine induced by interferon-γ) were not detected. Abbreviations: +, expression; −, no expression; CTACK, cutaneous T-cell attracting chemokine; IFS, immunofluorescence staining; MIP, macrophage inflammatory protein; N, normal skin; RT-PCR, reverse transcription-polymerase chain reaction; SDF, stromal cell-derived factor; SLC, secondary lymphoid tissue chemokine; W, wounded skin.

tissue injury, which could induce a greater accumulation of tissue-specific BM progenitor cells through tissue-specific chemokine/chemokine receptor interactions. To test this possibility in skin, we first examined the expression of a panel of chemokines as possible candidates by RT-PCR, Western blot analysis, and immunofluorescence staining (Table 1). RT-PCR and Western blot analyses were performed with normal skin or with skin 24 hours after wounding, including both epidermis and dermis. Experiments using RT-PCR (Fig. 1B) and Western blot analyses (Fig. 1C) showed that SDF-1α, SLC, and CTACK/CCL27 were constitutively expressed in normal skin and also wounded skin. Only CTACK expression was upregulated in wounded tissue. We examined the location of CTACK expressed in skin. Immunofluorescence staining demonstrated that CTACK expression was upregulated in the epidermis 3 days after wounding (Fig. 1D), whereas SDF-1α and SLC remained only weakly expressed (data not shown). Western blot analysis and immunofluorescence staining showed that MIP-1α and MIP-1β were not detectable, but RT-PCR analysis demonstrated a low level of expression of these chemokines. CTACK has recently been described in mice and humans as being exclusively expressed by keratinocytes [14]. CTACK selectively attracts cutaneous memory T cells [14] by interacting with a specific receptor, CCR10 [15]. CTACK/CCR10 interactions are directly involved in T-cell recruitment to inflamed skin [16]. However, there are no reports that suggest that this interaction is important for other cell types.

CXCR4, CCR7, and CCR10 Expression Were Detected on CD34$^+$ BM Cells

If chemokine/chemokine receptor interactions contribute to the recruitment of BM-derived tissue-specific precursor cells in damaged tissue, a specific chemokine should be upregulated in the target tissue together with a partner receptor expressed on the BM-derived tissue precursor cells. Although the markers identifying keratinocyte precursor cells in BM are still unknown, we chose CD34 as a stem cell marker; CD34 is a known marker for several BM precursor cell populations, including myocytes and neural cells [17, 18]. Expression of CXCR4, CCR7, and CCR10, which are specific receptors for the skin chemokines expressed in wounds (SDF-1α, SLC, and CTACK, respectively), were also analyzed together with CD34$^+$ BM cells using flow cytometry.

Approximately 19.1% of CD34$^+$ BM cells expressed CCR10 (Fig. 2A). In addition, CXCR4 and CCR7 were expressed in 97.4% and 12.9% on the CD34$^+$ cells, respectively (Fig. 2A).

CD34$^+$ BM Cells Migrated in Response to SDF-1α, SLC, and CTACK In Vitro

To confirm that these receptors were actually functional in these cells, in vitro chemotaxis assays were undertaken. CTACK induced CD34$^+$ BM cell migration in a dose-dependent manner (Fig. 2B, 2C). SDF-1α was previously known to induce hematopoietic stem cell migration via CXCR4 interactions [19]. Indeed, SDF-1α enhanced the migration of CD34$^+$ BM cells in a dose-dependent manner (Fig. 2B and data not shown). In addition, SLC enhanced CD34$^+$ BM cell migration (Fig. 2B and data not shown).

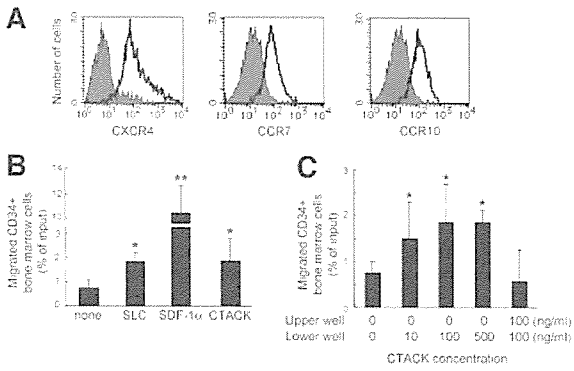

Figure 2. CCR10, a receptor for CTACK, was expressed in $CD34^+$ bone marrow (BM) cells and these $CD34^+$ BM cells migrated in response to CTACK in vitro. **(A):** Expression of CXCR4, a receptor for SDF-1α; CCR7, a receptor for SLC; and CCR10 on $CD34^+$ BM cells was analyzed by flow cytometry. Shown are the staining with a specific antibody for each chemokine receptor (solid line) and the background staining with the nonspecific immunoglobulin antibody (negative isotype-matched control; shaded profile) by the gated $CD34^+$ population. $CD34^+$ BM cells expressed CXCR4 (97.4%), CCR7 (12.9%), and CCR10 (19.1%). **(B, C):** Chemotaxis assays were undertaken in vitro. Isolated $CD34^+$ BM cells purified by fluorescence-activated cell sorting were added to the upper well of a 3-μm-pore Transwell. Recombinant SLC, SDF-1α, or CTACK was added to the upper and/or lower plate. $CD34^+$ BM cell migration rates increased in response to medium containing recombinant SLC, SDF-1α, or CTACK (100 ng/ml) ($* p < .05$, $** p < .001$) versus medium alone ($n = 4$) **(B)**. CTACK (0–500 ng/ml) induced $CD34^+$ BM cell migration in dose-dependent manner ($n = 4$) ($* p < .05$) **(C)**. SDF-1α and SLC also induced in dose-dependent manner (data not shown). Abbreviations: CTACK, cutaneous T-cell attracting chemokine; SDF-1α, stromal cell-derived factor-1α; SLC, secondary lymphoid tissue chemokine.

CTACK Treatment Specifically Led to Accumulations of BMDKs in Wounded Skin

To assess the ability of chemokines in keratinocyte precursor cell recruitment in vivo, we injected these chemokines to the periphery of wounded skin in enhanced GFP transgenic transplanted mice. The number of GFP-positive BMDKs in the epidermis was calculated ($n = 5$ mice in each group). Although SDF-1α and SLC failed to influence the number of BMDKs compared with the controls, CTACK significantly increased the number of BMDKs in wounded skin (Fig. 3A). Next, to clarify whether this increase of $CD34^+$ BM cells could enhance the overall number of BMDKs, we attempted to increase the levels of $CD34^+$ BM cells in peripheral blood by means of cytokine mobilization using G-CSF (five mice) or $CD34^+$ cell adoptive transfer (five mice). Increased numbers of $CD34^+$ BM cells in peripheral blood significantly enhanced the number of BMDKs in wounded skin in each group. In addition, CTACK treatment in this group significantly increased the number of BMDKs by approximately fivefold compared with the controls in each group (Fig. 3A). Furthermore, intradermal injection of CTACK neutralizing antibody inhibited this BMDK migration in a dose-dependent manner (five mice) (Fig. 3B).

CTACK Treatment Accelerated BMDK-Induced Wound Healing

We determined that CTACK was capable of inducing additional BMDKs that could participate in the host skin wound response. Surprisingly, intradermal injection of CTACK significantly accelerated wound closure (six mice) (Fig. 4A, 4B). We speculated that this effect was mediated by increases in BMDK. However, there are several possible reasons why intradermal injection of CTACK might accelerate wound repair. This could represent increased angiogenesis, keratinocyte proliferation, or keratinocyte migration during wound healing. Therefore, the following additional experiments were performed. We examined whether CTACK induced angiogenesis in wound healing. Three days after skin wounding, when the greatest number of new capillaries were formed [20], the number of dermal capillaries was calculated on two sections from each mouse (five mice per treatment group) and on an identical wound site section with or without CTACK injection (PBS vehicle control). CTACK had no effect on angiogenesis in wounded skin (Fig. 4C). Next, to determine whether CTACK induced keratinocyte proliferation, we measured proliferation rates in vitro. CTACK had no effect on the proliferation of the keratinocytes (six mice) (Fig. 4D). It has previously been reported that CCR10 is expressed on only skin-homing memory T cells. In our study, we confirmed that keratinocytes and fibroblasts in normal and wounded skin did not express CCR10 (data not shown). Finally, to determine whether CTACK induced keratinocyte migration, we undertook a keratinocyte migration assay in vitro. CTACK had no effect on keratinocyte migration. These results indicate that intradermal injection of CTACK accelerated wound healing without influencing angiogenesis, keratinocyte proliferation, or migration.

Discussion

We have shown that CTACK is a major regulator of keratinocyte precursor cell migration from the BM to the skin. In this study, BM-derived cells were able to transdifferentiate into keratinocytes at the sites of skin wounds. Furthermore, we have shown that CTACK is specifically expressed in wounded skin and that $CD34^+$ BM cells express CCR10, the main CTACK receptor. Although the numbers of BMDKs in untreated skin wounds are extremely low, a combination of treatments to increase the number of peripheral blood $CD34^+$ BM-derived cells, together with intradermal injection of CTACK into the wounded skin periphery, resulted in a 10-fold increase of BMDK. Furthermore, an increase in circulating $CD34^+$ BM cells enhanced the number of BMDKs, suggesting that a significant number of $CD34^+$ cells are included in the BMDK precursor population. Intradermal injection of CTACK significantly accelerated wound closure via increased rates of BMDK accumulation. We concluded that small populations of the progenitor cells coexpressing CD34 and CCR10 exist, that a subset of these cells migrated to the epidermis in response to CTACK, and that these cells play important roles in skin wound healing and repair.

Tissue repair and regeneration after injury is thought to involve the selective recruitment of circulating or resident stem cell populations. Chemokine/chemokine receptor interactions are expected to contribute to these mechanisms of stem cell plasticity. However, only one chemokine/chemokine receptor interaction, the SDF-1α/CXCR4 interaction, has thus far been reported. The SDF-1α/CXCR4 interaction has been identified as a factor causing hematopoietic stem cell mobilization [19]; however, other tissue cells are recruited from the BM by this

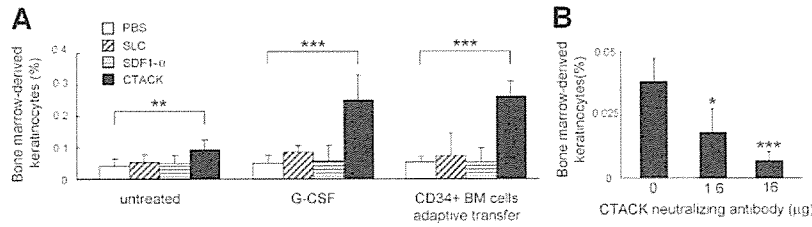

Figure 3. CTACK specifically accumulated bone marrow-derived keratinocytes (BMDKs) in wounded skin. **(A):** The number of BMDKs was quantified as a percentage of the total number of keratinocytes in wounded skin from untreated mice or those treated with G-CSF for cytokine mobilization or those that received $CD34^+$ BM cell adoptive transfer. SLC, SDF-1α, or CTACK (1 μg in 30 μl) was intradermally injected into the periphery of wounded skin (five mice in each group). CTACK significantly accumulated large numbers of BMDKs as compared with SLC, SDF-1α, and PBS (** $p < .01$). Furthermore, the number of BMDKs increased in mice treated with G-CSF for cytokine mobilization or those that received $CD34^+$ BM cell adoptive transfer (*** $p < .005$). **(B):** CTACK neutralizing antibody (0–16 μg in 120 μl) was injected to the periphery of wounded skin. The numbers of BMDKs were decreased by CTACK neutralizing antibody in dose-dependent manner (five mice) (* $p < .05$, *** $p < .005$). Abbreviations: BM, bone marrow; CTACK, cutaneous T-cell attracting chemokine; G-CSF, granulocyte colony stimulating factor; PBS, phosphate-buffered saline; SDF-1α, stromal cell-derived factor-1α; SLC, secondary lymphoid tissue chemokine.

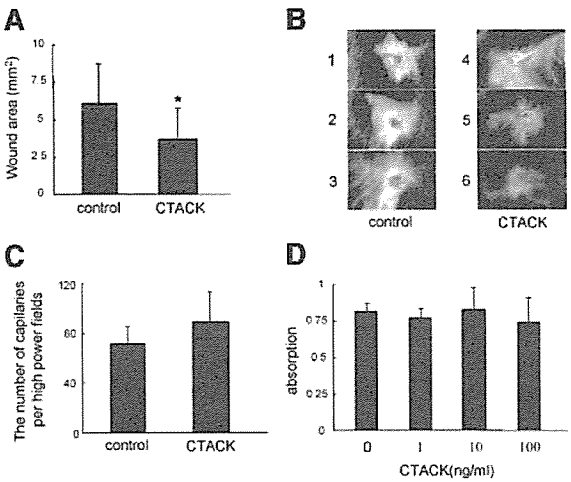

Figure 4. Increased bone marrow-derived keratinocytes (BMDKs) by CTACK accelerated wound closure without angiogenesis or keratinocyte proliferation. **(A, B):** Wound size was measured at 10 days after wounding and subsequent CTACK treatment (total 3 μg in 100 μl) or PBS (100 μl) as control (six mice in each group). Full-thickness cutaneous wounds were made and subsequently monitored daily. Intradermal injection of CTACK significantly accelerated wound closure (* $p < .05$) **(A)**. Representative images at 10 days after wounding of wounds treated with PBS (as control) (mice 1–3) or CTACK (mice 4–6) **(B)**. **(C):** The numbers of capillaries in the dermis treated by CTACK (1 μg in 30 μl) or PBS (30 μl) (as control vehicle) at 3 days after wounding were quantified. There was no statistical difference between CTACK and control (two sections each of five mice). **(D):** Keratinocytes were cultured with or without CTACK (0–100 ng/ml) for 72 hours, and viable cells were determined by proliferation assay. There was no statistical difference in proliferation of keratinocytes between the two treatment groups (nine mice). Abbreviations: CTACK, cutaneous T-cell attracting chemokine; PBS, phosphate-buffered saline.

interaction, including myocytes [21] and neural cells [22]. In addition, SDF-1α and CXCR4 are widely expressed on various cell types, and SDF-1α/CXCR4 interactions play an important role in several developmental and regenerative phenomena, such as cardiogenesis [21], neovascularization [23], hematopoiesis [19], and hepatic development [24]. Furthermore, wounding stimulated the engraftment of BM cells into the skin and induced BM-derived cells to incorporate into and differentiate into nonhematopoietic skin structures [25]. Given that it is unlikely that this receptor interaction is involved in many cell functions, organ-specific chemokine/chemokine receptor interactions are predicted. Indeed, we have demonstrated that the CTACK/CCR10 interaction is involved in skin wound healing. A strategy to detect further tissue-specific chemokines expressed in injured tissue would further benefit future organ-specific BM stem cell enrichment and recruitment.

Several studies have indicated that BM-derived cells have the ability to effect tissue regeneration in protein-deficient mouse models. Mice with damaged liver function caused by a fumarylacetoacetate hydrolase deficiency recovered after normal mouse-derived hematopoietic stem cell transplantation, in which mouse BM cells transdifferentiated into hepatocytes [26]. BM-derived cells may prove beneficial for protein-deficient disease therapy. In the study, the increase in BM-derived cells might further enhance the rate of damaged tissue recovery in wild-type mice. This suggests that cells derived from circulating stem cells are more effective at enlisting host regenerative mechanisms than resident tissue cells, indicating a promising therapeutic strategy for damaged tissues. Our results provide direct evidence that tissue-specific BM precursor cells are recruited with the help of tissue-specific chemokine/chemokine receptor interactions.

ACKNOWLEDGMENTS

This work was supported in part by grants-in-aid for Scientific Research (number 133,57008 to H.S. and number 157,90563 to R.A.) and the Project for Realization of Regenerative Medicine (to H.S.) from the Ministry of Education, Science, Sports, and Culture of Japan, and Health and Labor Sciences Research Grants (numbers H13-Measures for Intractable Disease-02 and H16-Measures for Intractable Disease-02 to H.S.) from the Ministry of Health, Labor, and Welfare of Japan. We thank Ayumi Honda for excellent technical assistance.

DISCLOSURES

The authors indicate no potential conflicts of interest.